
Surprisal-Rényi Free Energy

Shion Matsumoto*¹

Raul Castillo*¹

Benjamin Prada¹

Ankur Arjun Mali¹

¹Bellini College of Artificial Intelligence, Cybersecurity and Computing, University of South Florida, Tampa, Florida, USA

Abstract

The forward and reverse Kullback-Leibler (KL) divergences arise as limiting objectives in learning and inference yet induce markedly different inductive biases that cannot be explained at the level of expectations alone. In this work, we introduce the *Surprisal-Rényi Free Energy* (SRFE), a log-moment-based functional of the likelihood ratio that lies outside the class of f -divergences. We show that SRFE recovers forward and reverse KL divergences as singular endpoint limits and derive local expansions around both limits in which the variance of the log-likelihood ratio appears as a *first-order* correction. This reveals an explicit mean-variance tradeoff governing departures from KL-dominated regimes. We further establish a Gibbs-type variational characterization of SRFE as the unique minimizer of a weighted sum of KL divergences and prove that SRFE directly controls large deviations of excess code-length via Chernoff-type bounds, yielding a precise Minimum Description Length interpretation. Together, these results identify SRFE as a variance- and tail-sensitive free-energy functional that clarifies the geometric and large-deviation structure underlying forward- and reverse-KL limits, without unifying or subsuming distinct learning frameworks.

1 INTRODUCTION

Consider the task of approximating an intractable probability distribution $p(x)$ with a tractable probability distribution $q_\theta(x)$ parameterized by θ . The goal is to find the set of parameters $\theta \in \Theta$ that minimizes the divergence $D(p\|q_\theta)$. This basic formulation has been used in applications such as image classification [Krizhevsky et al., 2012], variational in-

ference [Kingma and Welling, 2022], generative adversarial networks [Goodfellow et al., 2014, Nowozin et al., 2016], knowledge distillation [Hinton et al., 2015], and reinforcement learning [Schulman et al., 2015, 2017, Ouyang et al., 2022]. While large families of divergences exist, probabilistic machine learning has been dominated by the (forward) Kullback-Leibler (KL) divergence $D_{\text{KL}}(P\|Q_\theta)$ [Kullback and Leibler, 1951] and its asymmetric counterpart, the reverse KL divergence $D_{\text{KL}}(Q_\theta\|P)$.

Perhaps the most classical use of the **forward KL** divergence is in supervised learning, where cross entropy is used as a proxy. The objective discourages q_θ from assigning small probability mass to samples it has observed, but in doing so, can assign probability mass to regions where samples do *not* exist in what is commonly referred to as **mass-covering** behavior [Minka, 2005]. In generative models, this can present itself in the generation of unrealistic samples with a high associated log-likelihood [Huszár, 2015, Theis et al., 2016].

In contrast, the **reverse KL** divergence forces q_θ to *avoid* assigning mass to regions where mass does *not* exist at the expense of failing to capture regions where mass does exist. This **mode-seeking** behavior results in q_θ collapsing onto a single mode of the distribution and ignoring regions with lower probability [Bishop, 2006]. A salient example of this is the training instability and collapse of generative adversarial networks towards a single point [Salimans et al., 2016]¹. More recently, similar phenomena have been observed in reinforcement learning fine-tuning for large language models [Li et al., 2025], perhaps due to the inherent bias of reverse KL divergence-based objectives [Schulman et al., 2017]. Fig. 1 illustrates the difference between mass-covering and mode-seeking behavior on a simple case of fitting a mixture of Gaussians with a single Gaussian.

We emphasize that the KL divergence is characterized by a

¹GANs originally used JSD as their objective but their collapsing behavior aligns with the mode-seeking behavior of the reverse KL divergence.

*Equal contribution.

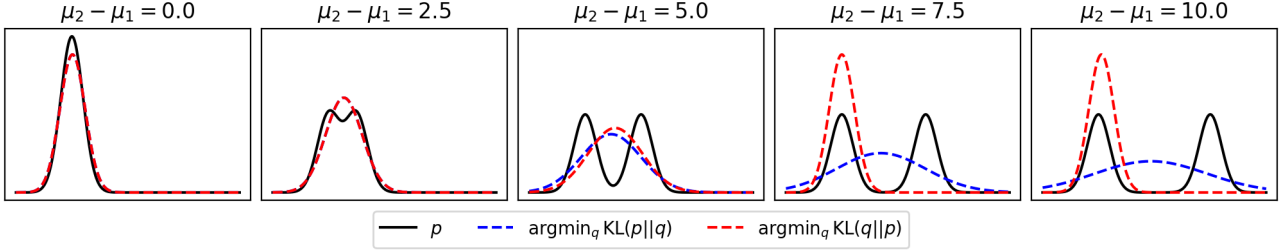


Figure 1: Gaussian Q that minimizes forward KL (blue) and reverse KL (red) with a mixture of Gaussians P with means μ_1, μ_2 where $\mu_2 \geq \mu_1$ and variance $\sigma_1^2 = \sigma_2^2 = 1$. Gaussians are equally weighted.

fundamental asymmetry: the forward and reverse KL divergences encode different inductive biases despite sharing the same global minimizer. This binarization of the choice of objective presents a fundamental limitation as models are destined toward either extrema when the optimal solution may lie in the middle.

Contribution Motivated by this limitation, we introduce the Surprisal-Rényi Free Energy (SRFE) – a risk-sensitive divergence between two probability distributions P and Q defined via a logarithmic interpolation between their densities. Formally, it is the scaled log moment-generating function (MGF) of the log-likelihood ratio $\log p(x)/q(x)$, which allows it to capture both average discrepancy and large-deviation behavior. A single parameter $\tau \in (0, 1)$ governs this interpolation: in the limit $\tau \rightarrow 0$, SRFE recovers the forward KL divergence $D_{\text{KL}}(P\|Q)$; in the limit $\tau \rightarrow 1$, it recovers the reverse KL divergence $D_{\text{KL}}(Q\|P)$. For intermediate values of τ , SRFE defines a smooth continuum between these two extremes, providing a tunable balance between average-case and tail-sensitive mismatch penalties.

In summary, our contributions are as follows:

1. We introduce the SRFE, a normalized log-moment-generating functional of the log-likelihood ratio, and establish its fundamental properties, including nonnegativity, KL limits, variational characterization, and its distinction from classical f -divergences (Section 3.1).
2. We perform a second-order analysis of SRFE around its KL limits, showing that while it shares local variance-of-surprisal corrections with power-divergence families, its curvature arises from a cumulant (log-MGF) structure rather than raw moment expansions (Section 3.2).
3. We derive the exact gradient form of SRFE and show that it admits an escort-distribution expectation representation, yielding a continuum between forward and reverse KL divergences and inducing distinct optimization dynamics and improved gradient conditioning (Section 3.3).
4. We prove that SRFE induces the Fisher-Rao Riemannian metric locally, demonstrating that it preserves the

intrinsic statistical manifold structure while modifying the global divergence geometry (Section 3.4).

5. We establish a minimum description length (MDL) interpretation of SRFE by deriving Chernoff-type tail bounds for excess codelength, showing that SRFE directly controls large-deviation behavior and risk-sensitive coding performance (Section 3.5).

2 PRELIMINARIES

Notation. Let P and Q denote probability distributions over a measurable space (\mathcal{X}, Σ) with densities $p(x)$ and $q_\theta(x)$ with respect to a σ -finite reference measure μ . We consider the task of approximating $p(x)$ using a parametric model $q_\theta(x)$ drawn from a predefined family (e.g., Gaussian). Our objective is to minimize a divergence measure $D(P\|Q_\theta)$. The forward KL divergence is defined as

$$D_{\text{KL}}(P\|Q) = \int_{\mathcal{X}} p(x) \log \frac{p(x)}{q_\theta(x)} d\mu(x), \text{ when } P \ll Q,$$

and the reverse KL divergence as

$$D_{\text{KL}}(Q\|P) = \int_{\mathcal{X}} q_\theta(x) \log \frac{q_\theta(x)}{p(x)} d\mu(x), \text{ when } Q \ll P.$$

2.1 f -DIVERGENCES

A broad class of divergences is given by the f -divergence family [Csiszár, 1963].

Definition 2.1 (f -divergence). Let $f : (0, \infty) \rightarrow \mathbb{R}$ be convex with $f(1) = 0$. The f -divergence from P to Q is

$$D_f(P\|Q) = \int_{\mathcal{X}} q(x) f\left(\frac{p(x)}{q(x)}\right) d\mu(x). \quad (1)$$

By appropriate choice of the generator f , this class recovers classical divergences such as the KL divergence, Jensen-Shannon divergence, χ^2 divergence, and Hellinger distance.

2.2 CRESSIE–READ POWER DIVERGENCE FAMILY

A notable one-parameter subset of f -divergences is the Cressie–Read (CR) power divergence family [Cressie and Read, 1984].

Definition 2.2 (Cressie–Read power divergence). Let $(\mathcal{X}, \Sigma, \mu)$ be a measure space and let P and Q be probability measures with densities $p = \frac{dP}{d\mu}$ and $q = \frac{dQ}{d\mu}$. Assume $P \ll Q$. For $\lambda \in \mathbb{R} \setminus \{0, -1\}$,

$$D_{\text{CR}}^\lambda(P\|Q) = \frac{1}{\lambda(\lambda+1)} \int_{\mathcal{X}} p(x) \left[\left(\frac{p(x)}{q(x)} \right)^\lambda - 1 \right] d\mu(x). \quad (2)$$

The cases $\lambda = 0$ and $\lambda = -1$ are defined by continuous limits.

The CR family was originally introduced for goodness-of-fit testing and provides a continuous interpolation between several classical divergences. Of particular interest here is its connection to the forward and reverse KL divergences.

Theorem 2.3 (CR limits to KL divergences). *Let P and Q be probability measures on a countable space.*

If $P \ll Q$, then

$$\lim_{\lambda \rightarrow 0} D_{\text{CR}}^\lambda(P\|Q) = D_{\text{KL}}(P\|Q).$$

If, in addition, $Q \ll P$, then

$$\lim_{\lambda \rightarrow -1} D_{\text{CR}}^\lambda(P\|Q) = D_{\text{KL}}(Q\|P).$$

Motivation for going beyond CR While CR offers a flexible interpolation between forward and reverse KL, it operates through power moments of the likelihood ratio p/q . Consequently, its behavior is governed by raw moment growth. In particular, heavy-tailed likelihood ratios can dominate the objective through high-order power terms. This observation motivates the development of alternative divergence constructions that operate on the logarithm of the moment-generating function, thereby inducing cumulant-based geometry and more direct control over tail behavior.

We refer readers to Appendix A for a brief overview of additional related work.

3 SURPRISAL-RÉNYI FREE ENERGY

In this paper, we propose the Surprisal–Rényi Free Energy (SRFE), a free energy functional based on the Rényi divergence. All proofs are included in Appendix B.

Definition 3.1 (SRFE and associated CR). Let $P, Q \ll \mu$ with densities $p = \frac{dP}{d\mu}$ and $q = \frac{dQ}{d\mu}$. Fix $\tau \in (0, 1)$ and define

$$F(\tau) := \int_{\mathcal{X}} p(x)^\tau q(x)^{1-\tau} d\mu(x), \quad (3)$$

which is the Chernoff τ -coefficient [Nielsen, 2011]. Assume $F(\tau) > 0$ so that the quantities below are finite.

1. The **Surprisal–Rényi Free Energy** is

$$D_{\text{SRFE}}^\tau(P\|Q) := \frac{-\log F(\tau)}{\tau(1-\tau)} \quad (4)$$

2. The **associated CR power divergence family** is

$$D_{\text{CR}}^\tau(P\|Q) := \frac{1-F(\tau)}{\tau(1-\tau)} \quad (5)$$

In particular, $D_{\text{CR}}^\tau(P\|Q)$ coincides with Definition 2.2 where $\lambda = \tau - 1$. See Section B.2 for derivation of Eq. (5). We will refer to the form introduced in Definition 2.2 as the standard CR and Definition 3.1 as the associated CR.

Almost disjoint supports Because of the $\log F(\tau)$ term in SRFE, it is *not* well-defined under *disjoint* supports. When p and q_θ share no overlap, $F(\tau) = 0$ for $\tau \in (0, 1)$ (hence $\log F(\tau) = -\infty$) and $F(\tau) = \infty$ for $\tau > 1$ (hence $\log F(\tau) = +\infty$), preventing gradient-based optimization. Importantly, $F(\tau) > 0$ does *not* require mutual absolute continuity ($p \ll q_\theta$ and $q_\theta \ll p$); it suffices that p and q_θ have *nonzero overlap* (i.e., the set $\{x : p(x) > 0, q_\theta(x) > 0\}$ has positive measure). In practice, model parameterizations and smoothing (e.g., softmax outputs, label smoothing, or additive density floors) typically ensure small but nonzero overlap allowing both SRFE and CR to be well-defined.

3.1 BASIC PROPERTIES

We summarize several key properties of SRFE.

Theorem 3.2 (KL limits). *For $\tau \in (0, 1)$ with $P \ll Q$ and $Q \ll P$,*

$$\begin{aligned} \lim_{\tau \rightarrow 0} D_{\text{SRFE}}^\tau(P\|Q) &= D_{\text{KL}}(P\|Q), \\ \lim_{\tau \rightarrow 1} D_{\text{SRFE}}^\tau(P\|Q) &= D_{\text{KL}}(Q\|P). \end{aligned}$$

Lemma 3.3 (Nonnegativity). *For $\tau \in (0, 1)$, we have $0 < F(\tau) \leq 1$, with equality $F(\tau) = 1$ if and only if $p = q$ μ -a.e. Consequently, $D_{\text{SRFE}}^\tau(P\|Q) \geq 0$ with equality if and only if $P = Q$.*

Lemma 3.4 (Monotone equivalence with CR). *For $\tau \in (0, 1)$, both CR and SRFE are strictly monotone transforms of the Chernoff τ -coefficient $F(\tau)$. Hence they induce identical orderings over models and share the same unique minimizer $p = q$.*

Therefore, while CR and SRFE agree at the level of model ordering, they differ structurally – whereas CR depends on raw power moments of the likelihood ratio, SRFE depends on the logarithm of the MGF.

Theorem 3.5 (SRFE is not an f -divergence). *For $\tau \in (0, 1)$, SRFE cannot be expressed in the form $\sum_i q_i f(p_i/q_i)$, and therefore is not an f -divergence.*

This distinction is significant: whereas CR belongs to the f -divergence family and is governed by power-moment behavior, SRFE operates on the logarithm of the MGF, thereby inducing a cumulant-based geometry. These properties establish that SRFE preserves the essential divergence characteristics of CR while departing structurally from the f -divergence class, thereby motivating separate geometric and optimization analysis.

3.2 SECOND-ORDER SURPRISAL ANALYSIS

We now compare the second-order behavior of CR and SRFE to provide further insight into their properties. For Theorems 3.6 to 3.8, we define the log-likelihood ratio (surprisal gap), $\Delta(x) := \log p(x)/q(x)$.

Theorem 3.6 (Surprisal-variance expansion for standard CR). *Let $P \ll Q$ and assume $\mathbb{E}_P[|\Delta|^3] < \infty$. For $\tau \neq 0, -1$ and the standard CR*

$$D_{\text{CR}}^\tau(P\|Q) := \frac{1}{\tau(\tau+1)} \int_{\mathcal{X}} p(x) \left[\left(\frac{p(x)}{q(x)} \right)^\tau - 1 \right] d\mu(x), \quad (6)$$

we have, as $\tau \rightarrow 0$,

$$D_{\text{CR}}^\tau(P\|Q) = D_{\text{KL}}(P\|Q) + \frac{\tau}{2} \text{Var}_P[\Delta] + \tau \left(\frac{1}{2} D_{\text{KL}}(P\|Q)^2 - D_{\text{KL}}(P\|Q) \right) + O(\tau^2). \quad (7)$$

In particular, the linear correction contains the term $\frac{\tau}{2} \text{Var}_P[\Delta]$.

We similarly perform a second-order (local) expansion of SRFE around the forward and reverse KL limits.

Theorem 3.7 (SRFE local expansion around forward KL). *Let $P \ll Q$ and assume $\mathbb{E}_P[\Delta^2] < \infty$ and that differentiation under the integral sign is permitted for*

$$F(\tau) := \int_{\mathcal{X}} p(x)^\tau q(x)^{1-\tau} d\mu(x) = \mathbb{E}_P \left[e^{-(1-\tau)\Delta(X)} \right] \quad (8)$$

in a neighborhood of $\tau = 1$. Then, as $\tau \uparrow 1$,

$$D_{\text{SRFE}}^\tau(P\|Q) = D_{\text{KL}}(P\|Q) + (1-\tau) \left(D_{\text{KL}}(P\|Q) - \frac{1}{2} \text{Var}_P[\Delta] \right) + O((1-\tau)^2). \quad (9)$$

Theorem 3.8 (SRFE local expansion around reverse KL). *Let $Q \ll P$ and assume $\mathbb{E}_P[\Delta^2] < \infty$ and that differentiation under the integral sign is permitted for*

$$F(\tau) := \int_{\mathcal{X}} p(x)^\tau q(x)^{1-\tau} d\mu(x) = \mathbb{E}_Q \left[e^{\tau\Delta(X)} \right] \quad (10)$$

in a neighborhood of $\tau = 0$. Then, as $\tau \downarrow 0$,

$$D_{\text{SRFE}}^\tau(P\|Q) = D_{\text{KL}}(Q\|P) + \tau \left(D_{\text{KL}}(Q\|P) - \frac{1}{2} \text{Var}_Q[\Delta] \right) + O(\tau^2). \quad (11)$$

Interpretation Equations (9) and (11) show that SRFE recovers $D_{\text{KL}}(P\|Q)$ as $\tau \uparrow 1$ and $D_{\text{KL}}(Q\|P)$ as $\tau \downarrow 0$, with a first-order correction proportional to the variance of the log-likelihood ratio $\Delta(x)$. This variance term captures second-order fluctuations of the excess codelength (surprisal) beyond the mean mismatch encoded by KL, and explains how τ tunes sensitivity to dispersion/tail behavior near the KL endpoints.

While the associated CR divergence also admits a second-order expansion involving the variance of the log-likelihood ratio, this variance arises from a power-moment expansion of the likelihood ratio. In contrast, SRFE is defined through the logarithm of the MGF, so its curvature is governed by cumulants of the log-likelihood ratio rather than raw moments. Consequently, although the local Taylor expansions of CR and SRFE contain similar variance terms, SRFE induces a different global geometry with direct connections to large-deviation behavior and tail sensitivity.

3.3 GRADIENT DYNAMICS

Next, we compare the learning dynamics for SRFE and CR, particularly in the almost disjoint setting, by deriving their gradients. For Lemmas 3.9 and 3.10, let q_θ be differentiable in θ and assume differentiation can be interchanged with integration.

Lemma 3.9 (SRFE gradient). *For $\tau \in (0, 1)$,*

$$\nabla_\theta D_{\text{SRFE}}^\tau(P\|Q_\theta) = -\frac{1}{\tau} \mathbb{E}_{x \sim r_\tau} [\nabla_\theta \log q_\theta(x)], \quad (12)$$

where

$$r_\tau(x) := \frac{p(x)^\tau q_\theta(x)^{1-\tau}}{F(\tau)}. \quad (13)$$

Lemma 3.10 (Associated CR gradient). *For $\tau \in (0, 1)$ and $u(x) = p(x)/q_\theta(x)$,*

$$\nabla_\theta D_{\text{CR}}^\tau(P\|Q_\theta) = -\frac{1}{\tau} \mathbb{E}_{x \sim Q_\theta} [u(x)^\tau \nabla_\theta \log q_\theta(x)]. \quad (14)$$

Equivalently (baseline-subtracted form),

$$\nabla_\theta D_{\text{CR}}^\tau(P\|Q_\theta) = -\frac{1}{\tau} \mathbb{E}_{x \sim Q_\theta} [(u(x)^\tau - 1) \nabla_\theta \log q_\theta(x)]. \quad (15)$$

Optimization advantages of SRFE Although SRFE does not eliminate the absolute-continuity requirement shared by divergence-based objectives, it offers distinct optimization advantages over classical f -divergences. Unlike CR or KL-type objectives, SRFE gradients do not contain explicit likelihood-ratio terms such as $u(x)^\tau$ inside the expectation; instead, the density ratio p/q influences optimization only through escort-distribution weights $r_\tau(x)$. For $\tau \in (0, 1)$, these weights suppress low-density regions of Q_θ , acting as an implicit trust region that prevents gradient amplification as $q_\theta(x) \rightarrow 0$. As a result, SRFE yields better-conditioned, lower-variance gradients in the almost disjoint regime and admits a continuous interpolation between conservative and aggressive update behavior via τ . These properties improve optimization stability without requiring ad-hoc clipping or regularization.

τ -scheduling The form of the SRFE gradient naturally lends itself to scheduling τ . Perhaps the simplest strategy is a linear schedule where $\tau \rightarrow 1$ and decreases to $\tau \rightarrow 0$. This gradually shifts SRFE from forward KL to reverse KL over the course of training, encouraging the model to first identify the support of the true distribution (mass-covering) and then learn the peaks (mode-seeking).

Next, we provide bounds on second moments. A finite second moment guarantees finite variance as $\text{Var}(g) \leq \mathbb{E}\|g\|^2$, while divergence of the second moment implies divergence of the variance. Second-moment bounds are therefore sufficient to characterize stability and avoid explicitly computing $\mathbb{E}[g]$, which is often intractable.

Lemma 3.11 (Associated CR gradient estimator and second-moment bound). *Let q_θ be a smooth density model and assume $\|\nabla_\theta \log q_\theta(x)\|^2 \leq C$ for all x . Fix $\tau \in (0, 1)$ and define $u(x) = p(x)/q_\theta(x)$. The unbiased one-sample stochastic gradient estimator for the associated CR under $X \sim Q_\theta$ is*

$$g_{\text{CR}}(X) := -\frac{1}{\tau} u(X)^\tau \nabla_\theta \log q_\theta(X). \quad (16)$$

Moreover,

$$\mathbb{E}_{X \sim Q_\theta}[\|g_{\text{CR}}(X)\|^2] \leq \frac{C}{\tau^2} \int_{\mathcal{X}} q_\theta(x) u(x)^{2\tau} d\mu(x), \quad (17)$$

which diverges whenever $q_\theta(x) \rightarrow 0$ on sets where $p(x) > 0$ and the integral is infinite.

Lemma 3.12 (SRFE gradient estimators and second-moment bounds). *Let q_θ be differentiable in θ and assume differentiation can be interchanged with integration. Fix $\tau \in (0, 1)$ and assume $\|\nabla_\theta \log q_\theta(x)\|^2 \leq C$ for all x . Define $F(\tau) = \int_{\mathcal{X}} p(x)^\tau q_\theta(x)^{1-\tau} d\mu(x)$, $r_\tau(x) = \frac{p(x)^\tau q_\theta(x)^{1-\tau}}{F(\tau)}$, and $u(x) = p(x)/q_\theta(x)$.*

(i) **Escort-sampling estimator.** If $X \sim r_\tau$, define

$$g_{\text{SRFE}}^{(r)}(X) := -\frac{1}{\tau} \nabla_\theta \log q_\theta(X). \quad (18)$$

Then $g_{\text{SRFE}}^{(r)}$ is unbiased for $\nabla_\theta D_{\text{SRFE}}^\tau(P\|Q_\theta)$ and satisfies

$$\mathbb{E}_{X \sim r_\tau}[\|g_{\text{SRFE}}^{(r)}(X)\|^2] \leq \frac{C}{\tau^2}. \quad (19)$$

(ii) **Q_θ -sampling (importance-weighted) estimator.** If $X \sim Q_\theta$, define

$$g_{\text{SRFE}}^{(q)}(X) := -\frac{1}{\tau} \frac{u(X)^\tau}{F(\tau)} \nabla_\theta \log q_\theta(X). \quad (20)$$

Then $g_{\text{SRFE}}^{(q)}$ is unbiased for $\nabla_\theta D_{\text{SRFE}}^\tau(P\|Q_\theta)$ and satisfies

$$\mathbb{E}_{X \sim Q_\theta}[\|g_{\text{SRFE}}^{(q)}(X)\|^2] \leq \frac{C}{\tau^2 F(\tau)^2} \int_{\mathcal{X}} q_\theta(x) u(x)^{2\tau} d\mu(x). \quad (21)$$

Fig. 2 illustrates the geometric difference between CR and SRFE gradients. When $p(x) > 0$ but $q_\theta(x) \rightarrow 0$, the density ratio $u(x)$ grows and causes the second moment (and hence the variance) of CR gradient estimators to diverge. In contrast, SRFE admits an escort-based estimator with uniformly bounded second moment, and even when expressed via Q_θ -sampling, its second moment is normalized by $F(\tau)^{-2}$. Consequently, in almost disjoint regimes, SRFE yields strictly better-conditioned gradient estimates, particularly for $\tau < \frac{1}{2}$.

3.4 INFORMATION-GEOMETRIC UNIFICATION

We now show that SRFE admits both a global and local information-geometric characterization.

Globally, SRFE can be expressed as a variational projection onto the exponential (Chernoff) path connecting P and Q [Nielsen, 2022]. For fixed $\tau \in (0, 1)$, $D_{\text{SRFE}}^\tau(P\|Q)$ equals a weighted KL projection onto an intermediate distribution $r_\tau \propto p^\tau q^{1-\tau}$. This distribution lies on the exponential geodesic between P and Q , and the resulting decomposition yields a Pythagorean identity in KL geometry (Fig. 7).

Locally, SRFE induces the same Riemannian metric as KL. The second-order expansion around $\theta' = \theta$ recovers the Fisher information matrix, independently of τ . Thus, although SRFE modifies the global geometry of the divergence landscape, it preserves the intrinsic statistical manifold structure.

Theorem 3.13 (Variational characterization of SRFE (information-geometric form)).

$$D_{\text{SRFE}}^\tau(P\|Q) = \min_{r \in \mathcal{P}(\mathcal{X})} \left\{ \frac{1}{\tau} D_{\text{KL}}(r\|Q) + \frac{1}{1-\tau} D_{\text{KL}}(r\|P) \right\}, \quad (22)$$

and the unique minimizer is the escort (Chernoff) distribution

$$r_\tau(x) = \frac{p(x)^\tau q(x)^{1-\tau}}{\int_{\mathcal{X}} p(u)^\tau q(u)^{1-\tau} d\mu(u)}. \quad (23)$$

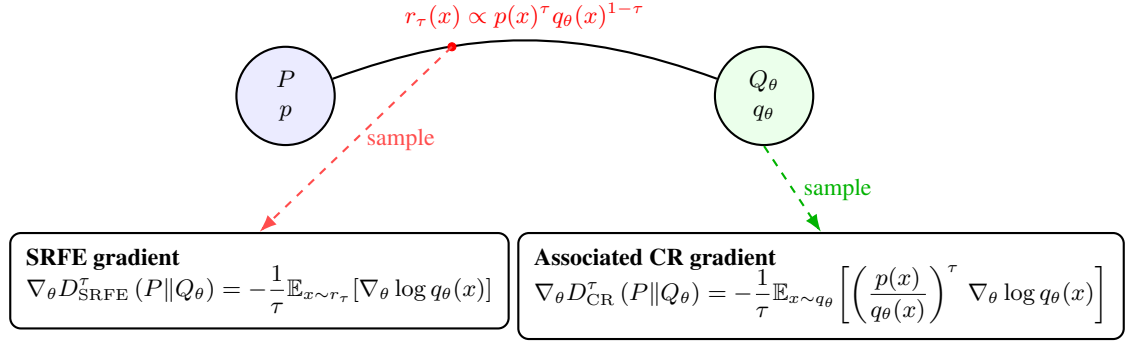


Figure 2: SRFE updates are driven by the score $\nabla_{\theta} \log q_{\theta}$ evaluated under the escort r_{τ} (which downweights regions where q_{θ} is small when $\tau \in (0, 1)$), whereas CR updates are driven by samples from q_{θ} with an explicit likelihood-ratio weight u^{τ} that can amplify variance when $q_{\theta} \ll p$.

Equivalently, the objective in Eq. (22) admits the decomposition

$$\frac{1}{\tau(1-\tau)} D_{\text{KL}}(r_{\tau} \| r_{\tau}) + D_{\text{SRFE}}^{\tau}(P \| Q), \quad (24)$$

which exhibits an information-geometric (Pythagorean) relation with projection onto the τ -escort path.

Theorem 3.14 (Riemannian metric induced by SRFE equals Fisher-Rao). *Let $\{p_{\theta} : \theta \in \Theta \subset \mathbb{R}^d\}$ be a smooth statistical model on $(\mathcal{X}, \Sigma, \mu)$ with strictly positive densities. Fix $\tau \in (0, 1)$ and define the SRFE divergence*

$$D_{\text{SRFE}}^{\tau}(p_{\theta} \| p_{\theta'}) := -\frac{1}{\tau(1-\tau)} \log \int_{\mathcal{X}} p_{\theta}(x)^{\tau} p_{\theta'}(x)^{1-\tau} d\mu(x). \quad (25)$$

Assume the usual regularity conditions allowing differentiation under the integral sign and the identities

$$\mathbb{E}_{\theta}[\partial_i \log p_{\theta}] = 0, \quad \mathbb{E}_{\theta}[\partial_{ij} \log p_{\theta}] = -I_{ij}(\theta),$$

where $I(\theta)$ is the Fisher information matrix

$$I_{ij}(\theta) := \mathbb{E}_{\theta}[\partial_i \log p_{\theta}(X) \partial_j \log p_{\theta}(X)].$$

Then the second-order expansion around $\theta' = \theta$ is

$$D_{\tau}^{\text{SRFE}}(p_{\theta} \| p_{\theta+\delta}) = \frac{1}{2} \delta^{\top} I(\theta) \delta + O(\|\delta\|^3). \quad (26)$$

Consequently, the Riemannian metric induced by SRFE,

$$g_{ij}^{(\text{SRFE})}(\theta) := \left. \frac{\partial^2}{\partial \theta^i \partial \theta^j} D_{\tau}^{\text{SRFE}}(p_{\theta} \| p_{\theta'}) \right|_{\theta'=\theta},$$

coincides with the Fisher-Rao metric:

$$g_{ij}^{(\text{SRFE})}(\theta) = I_{ij}(\theta). \quad (27)$$

Corollary 3.15 (τ -independence and Fisher-Rao unification). *Under the assumptions of Theorem 3.14, the Riemannian metric induced by D_{SRFE}^{τ} is independent of $\tau \in (0, 1)$ and equals the Fisher-Rao metric:*

$$g_{ij}^{(\text{SRFE})}(\theta) = I_{ij}(\theta) \quad \text{for all } \tau \in (0, 1).$$

Consequently, for any two smooth curves $\theta(t)$ and $\theta(t) + \delta(t)$ with $\delta(t) \rightarrow 0$, the SRFE locally induces the same infinitesimal squared distance as KL (and hence as any smooth f -divergence):

$$D_{\text{SRFE}}^{\tau}(p_{\theta} \| p_{\theta+\delta}) = \frac{1}{2} \delta^{\top} I(\theta) \delta + o(\|\delta\|^2),$$

uniformly over τ in compact subsets of $(0, 1)$.

3.5 MINIMUM DESCRIPTION LENGTH (MDL)

We now interpret SRFE through the lens of coding theory and large deviations. Recall that for densities p, q with $P \ll Q$, the log-likelihood ratio $\Delta(x)$ represents the *excess codelength* (in nats) incurred by encoding x with Q rather than the true distribution P .

Theorem 3.16 (SRFE controls large deviations of excess codelength). *Let $(\mathcal{X}, \Sigma, \mu)$ be a measurable space and let $P, Q \ll \mu$ with densities p, q . Fix $\tau \in (0, 1)$ and assume $F(\tau) = \int p(x)^{\tau} q(x)^{1-\tau} d\mu(x) \in (0, \infty)$. Then for any $a \in \mathbb{R}$,*

$$\Pr_{X \sim Q}[\Delta(X) \geq a] \leq \exp\left(-\tau a - \tau(1-\tau) D_{\text{SRFE}}^{\tau}(P \| Q)\right). \quad (28)$$

The bound in Eq. (28) is a Chernoff-type large-deviation inequality. Since

$$\tau(1-\tau) D_{\text{SRFE}}^{\tau}(P \| Q) = -\log \mathbb{E}_Q[e^{\tau \Delta}],$$

SRFE is precisely the normalized log-MGF of the excess codelength. Thus, SRFE controls the exponential rate at which unlikely compression advantages decay.

Gibbs (Chernoff) variational principle The SRFE admits the equivalent variational form

Theorem 3.17 (Gibbs variational characterization of SRFE). For fixed $\tau \in (0, 1)$ and $r \in \mathcal{P}(\mathcal{X})$

$$D_{\text{SRFE}}^\tau(P\|Q) = \min_r \left\{ \frac{1}{\tau} D_{\text{KL}}(r\|Q) + \frac{1}{1-\tau} D_{\text{KL}}(r\|P) \right\}, \quad (29)$$

with a unique minimizer $r_\tau(x)$.

This shows that SRFE corresponds to a weighted KL projection onto the exponential (Chernoff) path connecting P and Q . It therefore measures coding mismatch not only at the mean level (KL), but along the entire exponential family interpolation.

KL upper bounds For all $\tau \in (0, 1)$,

Corollary 3.18 (KL upper bounds for SRFE),

$$D_{\text{SRFE}}^\tau(P\|Q) \leq \frac{1}{1-\tau} D_{\text{KL}}(P\|Q), \quad (30)$$

$$D_{\text{SRFE}}^\tau(P\|Q) \leq \frac{1}{\tau} D_{\text{KL}}(Q\|P). \quad (31)$$

Equivalently,

$$D_{\text{SRFE}}^\tau(P\|Q) \leq \min \left\{ \frac{1}{1-\tau} D_{\text{KL}}(P\|Q), \frac{1}{\tau} D_{\text{KL}}(Q\|P) \right\}.$$

Thus, SRFE is uniformly controlled by both oriented KL divergences while retaining additional tail sensitivity.

MDL interpretation. Define Shannon codelengths

$$\ell_P(x) := -\log p(x), \quad \ell_Q(x) := -\log q(x).$$

Then the excess codelength incurred by using Q instead of P is

$$\ell_Q(x) - \ell_P(x) = \Delta(x).$$

Corollary 3.19 (MDL interpretation: exponential tail control). Let $\Delta(x) = \log \frac{p(x)}{q(x)}$. For any $a \in \mathbb{R}$,

$$\Pr_{X \sim Q} [\Delta(X) \geq a] \leq \exp \left(-\tau a - \tau(1-\tau) D_{\text{SRFE}}^\tau(P\|Q) \right). \quad (32)$$

Equivalently, the probability that model Q yields a description at least a nats longer than P decays exponentially at a rate governed by $D_{\text{SRFE}}^\tau(P\|Q)$.

Implications for deep networks. In deep neural networks, training via maximum likelihood minimizes $D_{\text{KL}}(P\|Q_\theta)$, which controls average excess codelength. However, Eq. (32) shows that SRFE additionally controls *rare but extreme miscalibration events* in which the model assigns exponentially too little probability to true outcomes.

Because SRFE is the log-moment-generating function of the log-likelihood ratio, it penalizes heavy tails in $\Delta(x)$ and thus discourages overconfident errors. This provides a principled connection between SRFE, calibration, and robustness, particularly in overparameterized deep models where rare catastrophic likelihood errors dominate downstream risk.

4 EXPERIMENTS

We conduct four controlled experiments to evaluate SRFE empirically and validate our theoretical results. All experiments train a single Gaussian model q_θ to approximate a mixture of three Gaussians. Since a unimodal Gaussian cannot represent a multimodal mixture exactly, the task forces explicit trade-offs between mode coverage and concentration. The setup for each experiment is outlined in Appendix D. Experiments were implemented in PyTorch on a single NVIDIA A6000 GPU.

We report mode coverage (number of mixture components assigned significant mass), effective sample size (ESS), test log-likelihood, and entropy error (absolute difference between model and true entropy). We refer readers to Appendix E for additional details on our results.

Experiment 1: Interpolation Between KL Objectives

We compare forward KL, reverse KL, and SRFE for $\tau \in \{0.1, 0.3, 0.5, 0.7, 0.9\}$. Contour plots and training curves (Fig. 3) show a continuous interpolation: large τ behaves similarly to forward KL (mean-seeking), while small τ resembles reverse KL (mode-seeking). This confirms the theoretical limit behavior of SRFE.

Experiment 2: Trade-offs Across τ

We sweep $\tau \in \{0.1, \dots, 0.9\}$ and evaluate the resulting models. A clear transition occurs near $\tau = 0.2$ to 0.3 (Fig. 4), where mode coverage, ESS, and test log-likelihood shift from concentration-dominated to dispersion-dominated behavior. This aligns with the curvature analysis showing that τ controls the bias-variance trade-off.

Experiment 3: Fixed vs Dynamic τ

We compare fixed $\tau \in \{0.01, 0.5, 0.99\}$ against various schedules for τ (linear/stepwise increase from $0.3 \rightarrow 0.9$, linear decrease from $0.9 \rightarrow 0.3$). Large fixed τ achieves the lowest final loss but exhibits early instability; small τ is stable but converges to higher loss. Overall, scheduling combines early stability with strong final performance (Fig. 5 and Table 5), consistent with the gradient-conditioning analysis.

Experiment 4: Robustness Under Contamination

We introduce increasing outlier contamination and train with $\tau \in \{0.01, 0.5, 0.9\}$. Lower τ values demonstrate greater robustness to contamination, exhibiting reduced entropy error growth and improved concentration control (Fig. 6). This

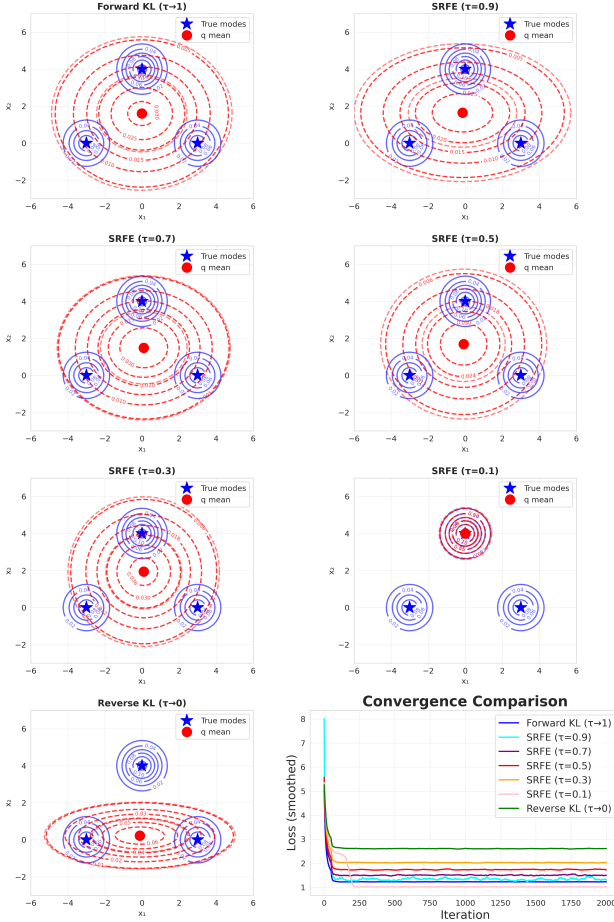


Figure 3: Experiment 1 - $\tau \in \{0.3, 0.5, 0.7, 0.9\}$ tends to spread out, matching Forward KL performance; $\tau \in \{0.1\}$ and Reverse KL hone in on fewer modes.

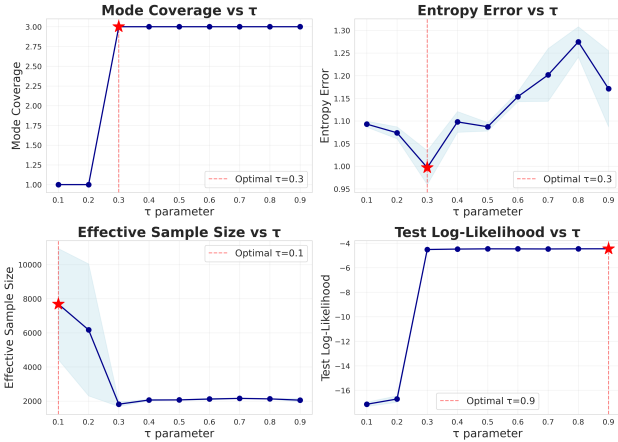


Figure 4: Experiment 2 - τ -sweep for τ with optimal mode coverage, entropy error, effective sample size, and test log-likelihood (in red).

matches the MDL interpretation that SRFE penalizes heavy-tailed likelihood ratios and controls rare extreme errors.

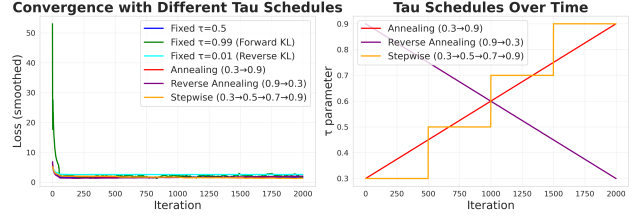


Figure 5: Experiment 3 - Fixed $\tau = 0.99$ schedule is unstable when compared to the other schedules

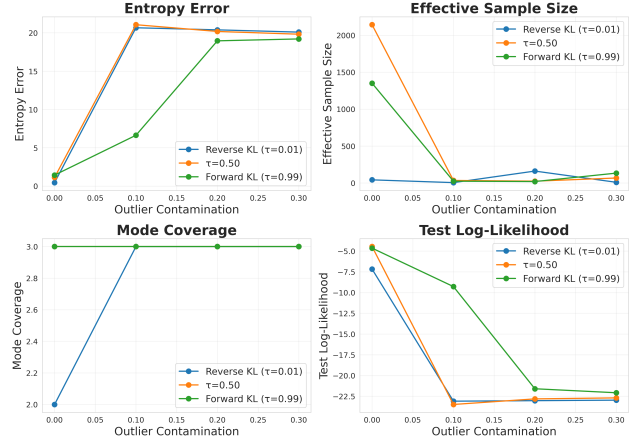


Figure 6: Experiment 4 - Entropy error, effective sample size, and test log-likelihood worsen as outlier contamination grows. Mode coverage improves.

5 CONCLUSION

We introduce the Surprisal-Rényi Free Energy (SRFE), a divergence that interpolates between forward and reverse KL while preserving the Fisher-Rao local geometry. Unlike classical f -divergences such as Cressie-Read, SRFE arises from a log-moment generating functional, making higher-order fluctuations of the log-likelihood ratio explicit and inducing a cumulant-based geometry. This structure yields improved gradient conditioning under near-support mismatch and provides a tunable mechanism for controlling mass-covering versus mode-seeking behavior via a single parameter τ . Empirical results on multimodal targets confirm that SRFE enables smooth interpolation between these regimes and that scheduling τ can improve optimization stability. Together, these results position SRFE as a principled objective for robust and risk-sensitive generative modeling.

References

Martin Arjovsky and Leon Bottou. Towards principled methods for training generative adversarial networks. In *International Conference on Learning Representations*, 2017. URL https://openreview.net/forum?id=Hk4_qw5xe.

- Christopher M. Bishop. *Pattern recognition and machine learning*. Springer Science + Business Media, 2006. ISBN 9780387310732.
- Noel Cressie and Timothy R C Read. Multinomial goodness-of-fit tests. *Journal of the Royal Statistical Society: Series B (Methodological)*, 46:440–464, 7 1984. ISSN 0035-9246. doi: 10.1111/j.2517-6161.1984.tb01318.x. URL <https://doi.org/10.1111/j.2517-6161.1984.tb01318.x>.
- Imre Csiszár. Eine informationstheoretische ungleichung und ihre anwendung auf den beweis der ergodizität von markoffschen ketten. *A Magyar Tudományok Akadémia Matematikai Kutató Intézetének Közleményei*, 8(1-2):85–108, 1963.
- Jacob Deasy, Nikola Simidjievski, and Pietro Lió. Constraining variational inference with geometric jensen-shannon divergence. In H Larochelle, M Ranzato, R Hadsell, M F Balcan, and H Lin, editors, *Advances in Neural Information Processing Systems*, volume 33, pages 10647–10658. Curran Associates, Inc., 2020. URL https://proceedings.neurips.cc/paper_files/paper/2020/file/78719f11fa2df9917de3110133506521-Paper.pdf.
- Ian J. Goodfellow, Jean Pouget-Abadie, Mehdi Mirza, Bing Xu, David Warde-Farley, Sherjil Ozair, Aaron Courville, and Yoshua Bengio. Generative adversarial nets. In Z. Ghahramani, M. Welling, C. Cortes, N. Lawrence, and K.Q. Weinberger, editors, *Advances in Neural Information Processing Systems*, volume 27. Curran Associates, Inc., 2014. URL https://proceedings.neurips.cc/paper_files/paper/2014/file/f033ed80deb0234979a61f95710dbe25-Paper.pdf.
- Jose Hernandez-Lobato, Yingzhen Li, Mark Rowland, Thang Bui, Daniel Hernandez-Lobato, and Richard Turner. Black-box alpha divergence minimization. In Maria Florina Balcan and Kilian Q. Weinberger, editors, *Proceedings of The 33rd International Conference on Machine Learning*, volume 48 of *Proceedings of Machine Learning Research*, pages 1511–1520, New York, New York, USA, 20–22 Jun 2016. PMLR. URL <https://proceedings.mlr.press/v48/hernandez-lobatob16.html>.
- Geoffrey Hinton, Oriol Vinyals, and Jeff Dean. Distilling the knowledge in a neural network, 2015. URL <https://arxiv.org/abs/1503.02531>.
- Ferenc Huszár. How (not) to train your generative model: Scheduled sampling, likelihood, adversary?, 2015. URL <https://arxiv.org/abs/1511.05101>.
- Juno Kim, Jaehyuk Kwon, Mincheol Cho, Hyunjong Lee, and Joong-Ho Won. t^3 -variational autoencoder: Learning heavy-tailed data with student’s t and power divergence. *The Twelfth International Conference on Learning Representations*, 3 2024. URL <http://arxiv.org/abs/2312.01133>.
- Diederik P Kingma and Max Welling. Auto-encoding variational bayes, 2022. URL <https://arxiv.org/abs/1312.6114>.
- Alex Krizhevsky, Ilya Sutskever, and Geoffrey E Hinton. Imagenet classification with deep convolutional neural networks. In F Pereira, C J Burges, L Bottou, and K Q Weinberger, editors, *Advances in Neural Information Processing Systems*, volume 25. Curran Associates, Inc., 2012. URL https://proceedings.neurips.cc/paper_files/paper/2012/file/c399862d3b9d6b76c8436e924a68c45b-Paper.pdf.
- S Kullback and R A Leibler. On information and sufficiency. *The Annals of Mathematical Statistics*, 22:79 – 86, 1951. doi: 10.1214/aoms/1177729694. URL <https://doi.org/10.1214/aoms/1177729694>.
- Long Li, Jiaran Hao, Jason Klein Liu, Zhijian Zhou, Yanting Miao, Wei Pang, Xiaoyu Tan, Wei Chu, Zhe Wang, Shirui Pan, Chao Qu, and Yuan Qi. The choice of divergence: A neglected key to mitigating diversity collapse in reinforcement learning with verifiable reward, 2025. URL <https://arxiv.org/abs/2509.07430>.
- J. Lin. Divergence measures based on the shannon entropy. *IEEE Transactions on Information Theory*, 37(1):145–151, 1991. doi: 10.1109/18.61115.
- Tom Minka. Divergence measures and message passing. Technical Report MSR-TR-2005-173, January 2005. URL <https://www.microsoft.com/en-us/research/publication/divergence-measures-and-message-passing/>.
- Frank Nielsen. Chernoff information of exponential families. *CoRR*, abs/1102.2684, 2011. URL <http://arxiv.org/abs/1102.2684>.
- Frank Nielsen. An information-geometric characterization of chernoff information. *IEEE Signal Processing Letters*, 20(3):269–272, 2013. doi: 10.1109/LSP.2013.2243726.
- Frank Nielsen. Revisiting chernoff information with likelihood ratio exponential families. *Entropy*, 24(10): 1400, October 2022. ISSN 1099-4300. doi: 10.3390/e24101400. URL <http://dx.doi.org/10.3390/e24101400>.

Sebastian Nowozin, Botond Cseke, and Ryota Tomioka. f-gan: Training generative neural samplers using variational divergence minimization, 2016. URL <https://arxiv.org/abs/1606.00709>.

Long Ouyang, Jeff Wu, Xu Jiang, Diogo Almeida, Carroll L. Wainwright, Pamela Mishkin, Chong Zhang, Sandhini Agarwal, Katarina Slama, Alex Ray, John Schulman, Jacob Hilton, Fraser Kelton, Luke Miller, Maddie Simens, Amanda Askell, Peter Welinder, Paul Christiano, Jan Leike, and Ryan Lowe. Training language models to follow instructions with human feedback. In *Proceedings of the 36th International Conference on Neural Information Processing Systems, NIPS '22*, Red Hook, NY, USA, 2022. Curran Associates Inc. ISBN 9781713871088.

Tim Salimans, Ian Goodfellow, Wojciech Zaremba, Vicki Cheung, Alec Radford, and Xi Chen. Improved techniques for training gans, 2016. URL <https://arxiv.org/abs/1606.03498>.

John Schulman, Sergey Levine, Pieter Abbeel, Michael Jordan, and Philipp Moritz. Trust region policy optimization. In Francis Bach and David Blei, editors, *Proceedings of the 32nd International Conference on Machine Learning*, volume 37 of *Proceedings of Machine Learning Research*, pages 1889–1897, Lille, France, 07–09 Jul 2015. PMLR. URL <https://proceedings.mlr.press/v37/schulman15.html>.

John Schulman, Filip Wolski, Prafulla Dhariwal, Alec Radford, and Oleg Klimov. Proximal policy optimization algorithms. *CoRR*, abs/1707.06347, 2017. URL <http://arxiv.org/abs/1707.06347>.

L. Theis, A. van den Oord, and M. Bethge. A note on the evaluation of generative models. In *International Conference on Learning Representations*, Apr 2016. URL <http://arxiv.org/abs/1511.01844>.

Surprisal-Rényi Free Energy (Supplementary Material)

Shion Matsumoto^{†1}

Raul Castillo^{*1}

Benjamin Prada¹

Ankur Arjun Mali¹

¹Bellini College of Artificial Intelligence, Cybersecurity and Computing, University of South Florida, Tampa, Florida, USA

This supplementary material provides additional details for results in the main body of the paper. Section A contains related work, Section B contains proofs for all theoretical results, Section C contains additional figures, Section D contains details on the parameters of the empirical experiments, and Section E contains additional experimental results that were not presented in the paper.

A RELATED WORK

One solution to the asymmetry is the Jensen-Shannon divergence (JSD) [Lin, 1991]. Though the JSD is symmetric and, in theory, partially inherits the mass-covering and mode-seeking behaviors of the forward and reverse KL divergences, this is not the case in GANs, as it failed to enforce mass-covering behavior [Arjovsky and Bottou, 2017]. Variations of the JSD, such as the skew-geometric JSD in variational inference, have been shown to be effective, though their analysis was limited to multivariate Gaussians [Deasy et al., 2020].

Other prior work on parameterized divergences, such as the Cressie-Read power divergence (CR) family [Cressie and Read, 1984], has successfully interpolated the forward and reverse limits, though only at the level of the expectation. This fails to explicitly capture essential higher-order behavior such as the variance or tail sensitivity, which would empower learning distributions beyond mean-matching by considering fluctuations of the log-likelihood ratio.

The Chernoff information (also known as Chernoff divergence) between two distributions P and Q is defined as:

$$D_C(P\|Q) = -\log \min_{\alpha \in (0,1)} \int p(x)^\alpha q(x)^{1-\alpha} dx, \quad (33)$$

where the integral term, $\int p^\alpha q^{1-\alpha}$, is known as the Chernoff α -coefficient [Nielsen, 2011]. Nielsen [2011, 2013] studied the geometric structure of the divergence between distributions of the same exponential family and provided analytic expressions for determining optimal Chernoff coefficients α for single-parameter exponential families.

Previous works have studied the utility of such parametric divergences, most commonly in the context of variational inference, which provides a natural way to evaluate the effect of interpolating between the forward and reverse KL divergences [Hernandez-Lobato et al., 2016, Kim et al., 2024, Deasy et al., 2020].

B PROOFS

This section provides proofs of the theorems, lemmas, and corollaries presented in the paper. Each subsection begins with a copy of the statement followed by the proof.

^{*}Equal contribution.

[†]Equal contribution.

B.1 PROOF OF THEOREM 2.3

Theorem 2.3 (CR limits to KL divergences). *Let P and Q be probability measures on a countable space. If $P \ll Q$, then*

$$\lim_{\lambda \rightarrow 0} D_{\text{CR}}^\lambda (P \| Q) = D_{\text{KL}} (P \| Q).$$

If, in addition, $Q \ll P$, then

$$\lim_{\lambda \rightarrow -1} D_{\text{CR}}^\lambda (P \| Q) = D_{\text{KL}} (Q \| P).$$

For this proof, we consider the limits $\lambda \rightarrow 0$ and $\lambda \rightarrow -1$ individually. Each case follows the same three steps:

1. Find Taylor expansion of $r(x)^\lambda$
2. Substitute expansion into the expression for CR
3. Evaluate expression at limit

Proof. Let $r(x) := p(x)/q(x)$ and $\Delta(x) := \log r(x)$ and define the discrete CR based on Eq. (2):

$$D_{\text{CR}}^\lambda (P \| Q) = \frac{1}{\lambda(\lambda+1)} \sum_x p(x) \left[\left(\frac{p(x)}{q(x)} \right)^\lambda - 1 \right] = \frac{1}{\lambda(\lambda+1)} \sum_x p(x) [r(x)^\lambda - 1]. \quad (34)$$

Limit $\lambda \rightarrow 0$. Using the expansion $r(x)^\lambda = e^{\lambda\Delta(x)} = 1 + \lambda\Delta(x) + O(\lambda^2)$,

$$r(x)^\lambda - 1 = \lambda\Delta(x) + O(\lambda^2).$$

Substituting into the summation term of Eq. (34),

$$\sum_x p(x)(r(x)^\lambda - 1) = \lambda \sum_x p(x)\Delta(x) + O(\lambda^2).$$

The denominator satisfies $\lambda(\lambda+1) = \lambda + O(\lambda^2)$. Therefore

$$D_{\text{CR}}^\lambda (P \| Q) = \frac{\lambda \sum_x p(x)\Delta(x) + O(\lambda^2)}{\lambda + O(\lambda^2)} \xrightarrow{\lambda \rightarrow 0} \sum_x p(x)\Delta(x) = D_{\text{KL}} (P \| Q).$$

Limit $\lambda \rightarrow -1$. Write $\lambda = -1 + \mu$ with $\mu \rightarrow 0$. Then

$$r(x)^\lambda = r(x)^{-1+\mu} = r(x)^{-1} e^{\mu\Delta(x)} = \frac{1}{r(x)} \left(1 + \mu\Delta(x) + O(\mu^2) \right).$$

Thus

$$r(x)^\lambda - 1 = \frac{1}{r(x)} - 1 + \mu \frac{\Delta(x)}{r(x)} + O(\mu^2).$$

Multiplying by $p(x)$,

$$p(x)(r(x)^\lambda - 1) = p(x) \left(\frac{1}{r(x)} - 1 \right) + \mu p(x) \frac{\Delta(x)}{r(x)} + O(\mu^2).$$

Since $p(x)/r(x) = q(x)$, this becomes

$$p(x) \left(\frac{1}{r(x)} - 1 \right) = q(x) - p(x), \quad p(x) \frac{\Delta(x)}{r(x)} = q(x)\Delta(x).$$

Summing over x ,

$$\sum_x p(x)(r(x)^\lambda - 1) = \sum_x (q(x) - p(x)) + \mu \sum_x q(x)\Delta(x) + O(\mu^2).$$

Because $\sum_x p(x) = \sum_x q(x) = 1$, the first term is zero:

$$\sum_x p(x)(r(x)^\lambda - 1) = \mu \sum_x q(x)\Delta(x) + O(\mu^2).$$

The denominator satisfies

$$\lambda(\lambda + 1) = (-1 + \mu)\mu = -\mu + O(\mu^2).$$

Hence

$$D_{\text{CR}}^\lambda(P\|Q) = \frac{\mu \sum_x q(x)\Delta(x) + O(\mu^2)}{-\mu + O(\mu^2)} \xrightarrow{\mu \rightarrow 0} -\sum_x q(x)\Delta(x) = \sum_x q(x) \log \frac{q(x)}{p(x)} = D_{\text{KL}}(Q\|P).$$

□

B.2 PROOF OF EQUATION 5

Definition 3.1 (SRFE and associated CR). Let $P, Q \ll \mu$ with densities $p = \frac{dP}{d\mu}$ and $q = \frac{dQ}{d\mu}$. Fix $\tau \in (0, 1)$ and define

$$F(\tau) := \int_{\mathcal{X}} p(x)^\tau q(x)^{1-\tau} d\mu(x), \quad (3)$$

which is the Chernoff τ -coefficient [Nielsen, 2011]. Assume $F(\tau) > 0$ so that the quantities below are finite.

1. The **Surprisal-Rényi Free Energy** is

$$D_{\text{SRFE}}^\tau(P\|Q) := \frac{-\log F(\tau)}{\tau(1-\tau)} \quad (4)$$

2. The **associated CR power divergence family** is

$$D_{\text{CR}}^\tau(P\|Q) := \frac{1 - F(\tau)}{\tau(1-\tau)} \quad (5)$$

In particular, $D_{\text{CR}}^\tau(P\|Q)$ coincides with Definition 2.2 where $\lambda = \tau - 1$. See Section B.2 for derivation of Eq. (5). We will refer to the form introduced in Definition 2.2 as the standard CR and Definition 3.1 as the associated CR.

We provide the steps used to derive the associated CR divergence and show that it can be expressed using $F(\tau)$ as defined in Eq. (3). This allows for an easy comparison with the SRFE as presented in Definition 3.1.

Proof. Substituting $\lambda = \tau - 1$ into the standard CR in Eq. (2), we get

$$\begin{aligned} D_{\text{CR}}^\tau(P\|Q) &= \frac{1}{\tau(\tau-1)} \int_{\mathcal{X}} p(x) \left[\left(\frac{p(x)}{q(x)} \right)^{\tau-1} - 1 \right] dx \\ &= \frac{1}{\tau(\tau-1)} \int_{\mathcal{X}} p(x)^\tau q(x)^{1-\tau} - p(x) dx \\ &= \frac{1}{\tau(\tau-1)} \left[\int_{\mathcal{X}} p(x)^\tau q(x)^{1-\tau} dx - \int_{\mathcal{X}} p(x) dx \right] \\ &= \frac{1}{\tau(\tau-1)} \left[\int_{\mathcal{X}} p(x)^\tau q(x)^{1-\tau} dx - 1 \right] \\ &= \frac{1}{\tau(1-\tau)} \left[1 - \int_{\mathcal{X}} p(x)^\tau q(x)^{1-\tau} dx \right] \end{aligned}$$

Using the definition $F(\tau) = \int p(x)^\tau q(x)^{1-\tau}$, we get

$$\frac{1}{\tau(1-\tau)} \left[1 - \int_{\mathcal{X}} p(x)^\tau q(x)^{1-\tau} dx \right] = \frac{1 - F(\tau)}{\tau(1-\tau)},$$

giving the form in Eq. (5). □

B.3 PROOF OF THEOREM 3.2

Theorem 3.2 (KL limits). For $\tau \in (0, 1)$ with $P \ll Q$ and $Q \ll P$,

$$\begin{aligned}\lim_{\tau \rightarrow 0} D_{\text{SRFE}}^\tau(P\|Q) &= D_{\text{KL}}(P\|Q), \\ \lim_{\tau \rightarrow 1} D_{\text{SRFE}}^\tau(P\|Q) &= D_{\text{KL}}(Q\|P).\end{aligned}$$

As with the proofs showing the limits of CR equal the forward and reverse KL divergences in Section B.1, we consider the limits as $\tau \rightarrow 1$ and $\tau \rightarrow 0$ for SRFE.

Proof. For the following proofs, let $F(\tau) := \int_{\mathcal{X}} p(x)^\tau q(x)^{1-\tau} dx$ as in Eq. (3).

Limit $\tau \rightarrow 1$. We begin by differentiating $F(\tau)$ under the integral sign,

$$F'(\tau) = \int_{\mathcal{X}} p(x)^\tau q(x)^{1-\tau} \log \frac{p(x)}{q(x)} dx.$$

At $\tau = 1$, we have

$$F(1) = \int_{\mathcal{X}} p(x) dx = 1, \quad F'(1) = \int_{\mathcal{X}} p(x) \log \frac{p(x)}{q(x)} dx = D_{\text{KL}}(P\|Q).$$

A first-order Taylor expansion of $F(\tau)$ around $\tau = 1$ yields

$$\begin{aligned}F(\tau) &= F(1) + F'(1)(\tau - 1) + o(\tau - 1) \\ &= 1 - (1 - \tau)D_{\text{KL}}(P\|Q) + o(1 - \tau).\end{aligned}\tag{35}$$

Since $F(1) = 1$, write $F(\tau) = 1 + \delta(\tau)$, where $\delta(\tau) \rightarrow 0$ as $\tau \rightarrow 1$. From Eq. (35),

$$\delta(\tau) = -(1 - \tau)D_{\text{KL}}(P\|Q) + o(1 - \tau).$$

Using the Taylor series $\log(1 + x) = x + o(x)$ as $x \rightarrow 0$,

$$\begin{aligned}\log F(\tau) &= \log(1 + \delta(\tau)) \\ &= \delta(\tau) + o(\delta(\tau)) \\ &= -(1 - \tau)D_{\text{KL}}(P\|Q) + o(1 - \tau).\end{aligned}$$

Substituting into Eq. (4) gives

$$\begin{aligned}\lim_{\tau \rightarrow 1} D_{\text{SRFE}}^\tau(P\|Q) &= \lim_{\tau \rightarrow 1} -\frac{\log F(\tau)}{\tau(1 - \tau)} \\ &= \lim_{\tau \rightarrow 1} -\frac{-(1 - \tau)D_{\text{KL}}(P\|Q) + o(1 - \tau)}{\tau(1 - \tau)} \\ &= D_{\text{KL}}(P\|Q).\end{aligned}$$

Limit $\tau \rightarrow 0$. The argument is analogous. One shows that $F(0) = \int_{\mathcal{X}} q(x) dx = 1$ and

$$F'(0) = \int_{\mathcal{X}} q(x) \log \frac{p(x)}{q(x)} dx = -D_{\text{KL}}(Q\|P),$$

so that the Taylor expansion of $F(\tau)$ around $\tau = 0$ yields

$$\begin{aligned}F(\tau) &= F(0) + F'(0)(\tau) + o(\tau) \\ &= 1 - \tau D_{\text{KL}}(Q\|P) + o(\tau)\end{aligned}\tag{36}$$

Since $F(0) = 1$, write $F(\tau) = 1 + \delta(\tau)$, where $\delta(\tau) \rightarrow 0$ as $\tau \rightarrow 0$. From Eq. (36),

$$\delta(\tau) = -\tau D_{\text{KL}}(Q\|P) + o(\tau).$$

Using the Taylor series of $\log(1+x) = x + o(x)$ as $x \rightarrow 0$ again, we get

$$\begin{aligned} \log F(\tau) &= \log(1 + \delta(\tau)) \\ &= \delta(\tau) + o(\delta(\tau)) \\ &= -\tau D_{\text{KL}}(Q\|P) + o(\tau). \end{aligned} \tag{37}$$

Substituting Eq. (37) into Eq. (4) yields

$$\begin{aligned} \lim_{\tau \rightarrow 0} D_{\text{SRFE}}^{\tau}(P\|Q) &= \lim_{\tau \rightarrow 0} -\frac{\log F(\tau)}{\tau(1-\tau)} \\ &= \lim_{\tau \rightarrow 0} -\frac{-\tau D_{\text{KL}}(Q\|P) + o(\tau)}{\tau(1-\tau)} \\ &= D_{\text{KL}}(Q\|P). \end{aligned}$$

This shows that SRFE interpolates between forward and reverse KL. \square

B.4 PROOF OF LEMMA 3.3

Lemma 3.3 (Nonnegativity). *For $\tau \in (0, 1)$, we have $0 < F(\tau) \leq 1$, with equality $F(\tau) = 1$ if and only if $p = q$ μ -a.e. Consequently, $D_{\text{SRFE}}^{\tau}(P\|Q) \geq 0$ with equality if and only if $P = Q$.*

We prove that the SRFE satisfies the property of nonnegativity for all p, q with equality if and only if $p = q$.

Proof. Since p, q are densities, $p^{\tau} q^{1-\tau} \geq 0$ and $F(\tau) \geq 0$. Assume $p, q > 0$ on a common support set of positive μ -measure so that $F(\tau) > 0$ (otherwise SRFE is $+\infty$ by definition).

To prove the upper bound $F(\tau) \leq 1$, apply Hölder's inequality with exponents $a := \frac{1}{\tau} > 1$ and $b := \frac{1}{1-\tau} > 1$ so that $\frac{1}{a} + \frac{1}{b} = \tau + (1-\tau) = 1$. Write

$$p^{\tau} q^{1-\tau} = (p)^{\tau} (q)^{1-\tau}.$$

Then

$$\begin{aligned} F(\tau) &= \int p^{\tau} q^{1-\tau} d\mu \leq \left(\int (p^{\tau})^a d\mu \right)^{1/a} \left(\int (q^{1-\tau})^b d\mu \right)^{1/b} \\ &= \left(\int p d\mu \right)^{\tau} \left(\int q d\mu \right)^{1-\tau} = 1^{\tau} \cdot 1^{1-\tau} = 1. \end{aligned}$$

This proves $0 \leq F(\tau) \leq 1$.

For the equality condition: Hölder's inequality is tight if and only if there exists a constant $c > 0$ such that

$$(p^{\tau})^a = c (q^{1-\tau})^b \quad \mu\text{-a.e. on the common support.}$$

Since $(p^{\tau})^a = p$ and $(q^{1-\tau})^b = q$, this becomes $p = cq$ μ -a.e. Integrating both sides gives $1 = \int p d\mu = c \int q d\mu = c$, hence $c = 1$ and therefore $p = q$ μ -a.e. Conversely, if $p = q$ then $F(\tau) = \int p = 1$.

Finally, since $F(\tau) \in (0, 1]$, we have $\log F(\tau) \leq 0$, and because $\tau(1-\tau) > 0$, it follows that

$$D_{\text{SRFE}}^{\tau}(P\|Q) = -\frac{1}{\tau(1-\tau)} \log F(\tau) \geq 0,$$

with equality if and only if $F(\tau) = 1$, i.e. iff $p = q$ μ -a.e. \square

B.5 PROOF OF LEMMA 3.4

Lemma 3.4 (Monotone equivalence with CR). *For $\tau \in (0, 1)$, both CR and SRFE are strictly monotone transforms of the Chernoff τ -coefficient $F(\tau)$. Hence they induce identical orderings over models and share the same unique minimizer $p = q$.*

Proof. Rearranging Eq. (5), we get

$$D_{\text{CR}}^\tau(P\|Q) = \frac{1 - F(\tau)}{\tau(1 - \tau)} \implies F(\tau) = 1 - \tau(1 - \tau) D_{\text{CR}}^\tau(P\|Q).$$

Substituting this into the SRFE expression gives

$$D_{\text{SRFE}}^\tau(P\|Q) = -\frac{1}{\tau(1 - \tau)} \log(1 - \tau(1 - \tau) D_{\text{CR}}^\tau(P\|Q)).$$

Let

$$h_\tau(d) := -\frac{1}{\tau(1 - \tau)} \log(1 - \tau(1 - \tau)d),$$

for $d \in \left[0, \frac{1}{\tau(1 - \tau)}\right)$, then

$$D_{\text{SRFE}}^\tau(P\|Q) = h_\tau(D_{\text{CR}}^\tau(P\|Q)).$$

Since P and Q are mutually absolutely continuous, we have $F(\tau) \in (0, 1]$, hence

$$\tau(1 - \tau) D_{\text{CR}}^\tau(P\|Q) = 1 - F(\tau) \in [0, 1),$$

so h_τ is well-defined on $d \in \left[0, \frac{1}{\tau(1 - \tau)}\right)$. Differentiating $h_\tau(d)$ yields

$$h'_\tau(d) = -\frac{1}{\tau(1 - \tau)} \cdot \frac{-\tau(1 - \tau)}{1 - \tau(1 - \tau)d} = \frac{1}{1 - \tau(1 - \tau)d} > 0,$$

showing that h_τ is smooth and strictly increasing on its domain d .

Strict monotonicity implies

$$D_{\text{CR}}^\tau(P\|Q_1) < D_{\text{CR}}^\tau(P\|Q_2) \iff h_\tau(D_{\text{CR}}^\tau(P\|Q_1)) < h_\tau(D_{\text{CR}}^\tau(P\|Q_2)),$$

which gives the stated ordering for SRFE.

Finally, $F(\tau) = 1$ if and only if $p = q$ a.e., which gives

$$D_{\text{CR}}^\tau(P\|P) = 0 \quad \text{and} \quad D_{\text{SRFE}}^\tau(P\|P) = 0.$$

Since $F(\tau) \leq 1$, these are the global minimum values over P . This establishes the uniqueness of the common minimizer and completes the proof. \square

B.6 PROOF OF THEOREM 3.5

Theorem 3.5 (SRFE is not an f -divergence). *For $\tau \in (0, 1)$, SRFE cannot be expressed in the form $\sum_i q_i f(p_i/q_i)$, and therefore is not an f -divergence.*

To prove that SRFE is *not* an f -divergence, we use a proof by contradiction. We consider the simple case of a 2-simplex $\Delta^2 = \{(p_0, p_1, p_2) \in \mathbb{R}^3 \mid \sum_{i=0}^2 p_i = 1, p_i \geq 0 \text{ for } i = 0, 1, 2\}$ and assume that SRFE can be expressed as an f -divergence. We then compare its second derivative to the second derivative of the closed form SRFE on the 2-simplex case.

Proof. Assume for contradiction that there exists a generator f such that

$$D_{\text{SRFE}}^\tau(P\|Q) = \sum_{i=1}^3 q_i f\left(\frac{p_i}{q_i}\right) \quad \text{for all } p, q \in \Delta^2. \quad (38)$$

Fix $q = (1/3, 1/3, 1/3)$ and parameterize p by two free variables: for (u, v) in an open set where $u > 0$, $v > 0$, and $u + v < 1$, set

$$p(u, v) = (u, v, 1 - u - v).$$

Define the scalar function

$$G(u, v) := D_\tau^{\text{SRFE}}(p(u, v)\|q).$$

With uniform q , SRFE becomes

$$G(u, v) = -\frac{1}{\tau(1-\tau)} \log\left(3^{\tau-1}[u^\tau + v^\tau + (1-u-v)^\tau]\right) = C_\tau - \frac{1}{\tau(1-\tau)} \log S(u, v),$$

where $C_\tau := -\frac{\tau-1}{\tau(1-\tau)} \log 3$ is constant and

$$S(u, v) := u^\tau + v^\tau + (1-u-v)^\tau.$$

On the other hand, the assumed f -divergence representation Eq. (38) with $q_i = 1/3$ gives

$$G(u, v) = \frac{1}{3}f(3u) + \frac{1}{3}f(3v) + \frac{1}{3}f(3(1-u-v)).$$

Differentiate twice with respect to u and v . Since the first two terms depend only on u or only on v , the *mixed* second derivative comes only from the third term:

$$\frac{\partial^2 G}{\partial u \partial v}(u, v) = \frac{1}{3} \cdot f''(3(1-u-v)) \cdot (-3)(-3) = 3 f''(3(1-u-v)). \quad (39)$$

In particular, the mixed derivative depends *only on* $1-u-v$.

Now compute the mixed derivative from the SRFE closed form. Since $G(u, v) = C_\tau - \frac{1}{\tau(1-\tau)} \log S(u, v)$, we have

$$\frac{\partial^2 G}{\partial u \partial v} = -\frac{1}{\tau(1-\tau)} \left(\frac{S_{uv}}{S} - \frac{S_u S_v}{S^2} \right).$$

A direct computation gives, for $\tau \in (0, 1)$,

$$S_u = \tau u^{\tau-1} - \tau(1-u-v)^{\tau-1}, \quad S_v = \tau v^{\tau-1} - \tau(1-u-v)^{\tau-1},$$

and

$$S_{uv} = \tau(\tau-1)(1-u-v)^{\tau-2}.$$

Substituting yields

$$\frac{\partial^2 G}{\partial u \partial v}(u, v) = -\frac{1}{\tau(1-\tau)} \left(\frac{\tau(\tau-1)w^{\tau-2}}{S(u, v)} - \frac{(\tau u^{\tau-1} - \tau w^{\tau-1})(\tau v^{\tau-1} - \tau w^{\tau-1})}{S(u, v)^2} \right), \quad (40)$$

where $w := 1-u-v$.

Crucially, the right-hand side of Eq. (40) depends on u and v *separately* through the factors $u^{\tau-1}$ and $v^{\tau-1}$, not only through $w = 1-u-v$. Therefore, $\frac{\partial^2 G}{\partial u \partial v}(u, v)$ cannot be a function of w alone on any open set.

This contradicts Eq. (39), which implies the mixed derivative must be of the form $H(1-u-v) = H(w)$ for some one-variable function H .

Hence no such f exists and SRFE cannot be an f -divergence. \square

B.7 PROOF OF THEOREM 3.6

Theorem 3.6 (Surprisal-variance expansion for standard CR). *Let $P \ll Q$ and assume $\mathbb{E}_P[|\Delta|^3] < \infty$. For $\tau \neq 0, -1$ and the standard CR*

$$D_{\text{CR}}^\tau(P\|Q) := \frac{1}{\tau(\tau+1)} \int_{\mathcal{X}} p(x) \left[\left(\frac{p(x)}{q(x)} \right)^\tau - 1 \right] d\mu(x), \quad (6)$$

we have, as $\tau \rightarrow 0$,

$$D_{\text{CR}}^\tau(P\|Q) = D_{\text{KL}}(P\|Q) + \frac{\tau}{2} \text{Var}_P[\Delta] + \tau \left(\frac{1}{2} D_{\text{KL}}(P\|Q)^2 - D_{\text{KL}}(P\|Q) \right) + O(\tau^2). \quad (7)$$

In particular, the linear correction contains the term $\frac{\tau}{2} \text{Var}_P[\Delta]$.

Proof. Let $r(x) := p(x)/q(x) = e^{\Delta(x)}$. Then

$$D_{\text{CR}}^\tau(P\|Q) = \frac{1}{\tau(\tau+1)} \int p(x) (r(x)^\tau - 1) d\mu(x) = \frac{1}{\tau(\tau+1)} \int p(x) (e^{\tau\Delta(x)} - 1) d\mu(x).$$

Step 1: Taylor expansion of the numerator. By Taylor's theorem,

$$e^{\tau\Delta(x)} = 1 + \tau\Delta(x) + \frac{\tau^2}{2} \Delta(x)^2 + R_3(\tau, x),$$

where the remainder satisfies

$$|R_3(\tau, x)| \leq \frac{|\tau|^3}{6} |\Delta(x)|^3 e^{|\tau||\Delta(x)|}.$$

Under $\mathbb{E}_p[|\Delta|^3] < \infty$, for τ in a neighborhood of 0 the bound is p -integrable, so integrating termwise yields

$$\int p(x) (e^{\tau\Delta(x)} - 1) d\mu(x) = \tau \mathbb{E}_p[\Delta] + \frac{\tau^2}{2} \mathbb{E}_p[\Delta^2] + O(\tau^3).$$

Step 2: Divide by $\tau(\tau+1)$. Using $\tau(\tau+1) = \tau(1+\tau)$,

$$\begin{aligned} D_{\text{CR}}^\tau(P\|Q) &= \frac{\tau \mathbb{E}_p[\Delta] + \frac{\tau^2}{2} \mathbb{E}_p[\Delta^2] + O(\tau^3)}{\tau(1+\tau)} \\ &= \frac{\mathbb{E}_p[\Delta] + \frac{\tau}{2} \mathbb{E}_p[\Delta^2] + O(\tau^2)}{1+\tau}. \end{aligned}$$

Expanding $(1+\tau)^{-1} = 1 - \tau + O(\tau^2)$ (valid as $|\tau| < 1$) gives

$$D_{\text{CR}}^\tau(P\|Q) = \mathbb{E}_p[\Delta] + \tau \left(-\mathbb{E}_p[\Delta] + \frac{1}{2} \mathbb{E}_p[\Delta^2] \right) + O(\tau^2).$$

Step 3: Express in terms of KL and variance. Since $\mathbb{E}_p[\Delta] = D_{\text{KL}}(P\|Q)$ and $\mathbb{E}_p[\Delta^2] = \text{Var}_p[\Delta] + \mathbb{E}_p[\Delta]^2 = \text{Var}_p[\Delta] + D_{\text{KL}}(P\|Q)^2$, we obtain

$$\begin{aligned} D_{\text{CR}}^\tau(P\|Q) &= D_{\text{KL}}(P\|Q) + \tau \left(-D_{\text{KL}}(P\|Q) + \frac{1}{2} \text{Var}_p[\Delta] + \frac{1}{2} D_{\text{KL}}(P\|Q)^2 \right) + O(\tau^2) \\ &= D_{\text{KL}}(P\|Q) + \frac{\tau}{2} \text{Var}_p[\Delta] + \tau \left(\frac{1}{2} D_{\text{KL}}(P\|Q)^2 - D_{\text{KL}}(P\|Q) \right) + O(\tau^2), \end{aligned}$$

which is Eq. (7). □

B.8 PROOF OF THEOREM 3.7

Theorem 3.7 (SRFE local expansion around forward KL). *Let $P \ll Q$ and assume $\mathbb{E}_P[\Delta^2] < \infty$ and that differentiation under the integral sign is permitted for*

$$F(\tau) := \int_{\mathcal{X}} p(x)^\tau q(x)^{1-\tau} d\mu(x) = \mathbb{E}_P \left[e^{-(1-\tau)\Delta(X)} \right] \quad (8)$$

in a neighborhood of $\tau = 1$. Then, as $\tau \uparrow 1$,

$$D_{\text{SRFE}}^\tau(P\|Q) = D_{\text{KL}}(P\|Q) + (1-\tau) \left(D_{\text{KL}}(P\|Q) - \frac{1}{2} \text{Var}_P[\Delta] \right) + O((1-\tau)^2). \quad (9)$$

Proof. Let

$$Z(\tau) := \int p(x)^\tau q(x)^{1-\tau} dx, \quad F(\tau) := \log Z(\tau).$$

A second-order Taylor expansion of $F(\tau)$ at $\tau = 1$ gives

$$F(\tau) = F(1) + (\tau - 1)F'(1) + \frac{1}{2}(\tau - 1)^2 F''(1) + O((\tau - 1)^3). \quad (41)$$

We first compute $F'(1)$ and $F''(1)$. Differentiating $Z(\tau)$ under the integral sign,

$$\begin{aligned} Z'(\tau) &= \int \left(p(x)^\tau \log p(x) \right) q(x)^{1-\tau} dx + \int p(x)^\tau \left(q(x)^{1-\tau} (-\log q(x)) \right) dx \\ &= \int p(x)^\tau q(x)^{1-\tau} (\log p(x) - \log q(x)) dx \\ &= \int p(x)^\tau q(x)^{1-\tau} \Delta(x) dx, \end{aligned} \quad (42)$$

$$Z''(\tau) = \int p(x)^\tau q(x)^{1-\tau} \Delta(x)^2 dx. \quad (43)$$

Hence

$$F'(\tau) = \frac{Z'(\tau)}{Z(\tau)}, \quad F''(\tau) = \frac{Z(\tau)Z''(\tau) - Z'(\tau)^2}{Z(\tau)^2}.$$

At $\tau = 1$ we have $Z(1) = \int p(x) dx = 1$, and

$$\begin{aligned} F(1) &= \log Z(1) = 0, \\ F'(1) &= Z'(1) = \int p(x)\Delta(x) dx = \int p(x) \log \frac{p(x)}{q(x)} dx = D_{\text{KL}}(P\|Q), \\ F''(1) &= Z''(1) - Z'(1)^2 \\ &= \int p(x)\Delta(x)^2 dx - \left(\int p(x)\Delta(x) dx \right)^2 \\ &= \text{Var}_p[\Delta]. \end{aligned}$$

Substituting into Eq. (41) gives

$$F(\tau) = (\tau - 1)D_{\text{KL}}(P\|Q) + \frac{(\tau - 1)^2}{2} \text{Var}_p[\Delta] + O((\tau - 1)^3).$$

Factoring out $(\tau - 1)$, we get

$$F(\tau) = (\tau - 1) \left(D_{\text{KL}}(P\|Q) + \frac{\tau - 1}{2} \text{Var}_p[\Delta] + O((\tau - 1)^2) \right).$$

Since $\tau(1 - \tau) = -\tau(\tau - 1)$, we obtain

$$D_{\text{SRFE}}^\tau(P\|Q) = -\frac{F(\tau)}{\tau(1 - \tau)} = -\frac{\tau - 1}{\tau(1 - \tau)} \left(D_{\text{KL}}(P\|Q) + \frac{\tau - 1}{2} \text{Var}_p[\Delta] + O((\tau - 1)^2) \right).$$

Note that

$$-\frac{\tau - 1}{\tau(1 - \tau)} = \frac{1}{\tau} \cdot \frac{1 - \tau}{1 - \tau} = \frac{1}{\tau},$$

so

$$D_{\text{SRFE}}^\tau(P\|Q) = \frac{1}{\tau} \left(D_{\text{KL}}(P\|Q) + \frac{\tau - 1}{2} \text{Var}_p[\Delta] + O((\tau - 1)^2) \right).$$

Now expand $1/\tau$ around $\tau = 1$:

$$\frac{1}{\tau} = \frac{1}{1 + (\tau - 1)} = 1 - (\tau - 1) + O((\tau - 1)^2).$$

Thus

$$\begin{aligned} D_{\text{SRFE}}^\tau(P\|Q) &= \left(1 - (\tau - 1) + O((\tau - 1)^2) \right) \left(D_{\text{KL}}(P\|Q) + \frac{\tau - 1}{2} \text{Var}_p[\Delta] + O((\tau - 1)^2) \right) \\ &= D_{\text{KL}}(P\|Q) + (\tau - 1) \left(-D_{\text{KL}}(P\|Q) + \frac{1}{2} \text{Var}_p[\Delta] \right) + O((\tau - 1)^2), \\ &= D_{\text{KL}}(P\|Q) + (1 - \tau) \left(D_{\text{KL}}(P\|Q) - \frac{1}{2} \text{Var}_p[\Delta] \right) + O((\tau - 1)^2), \end{aligned}$$

which is exactly Eq. (9). □

B.9 PROOF OF THEOREM 3.8

Theorem 3.8 (SRFE local expansion around reverse KL). *Let $Q \ll P$ and assume $\mathbb{E}_P[\Delta^2] < \infty$ and that differentiation under the integral sign is permitted for*

$$F(\tau) := \int_{\mathcal{X}} p(x)^\tau q(x)^{1-\tau} d\mu(x) = \mathbb{E}_Q \left[e^{\tau \Delta(X)} \right] \quad (10)$$

in a neighborhood of $\tau = 0$. Then, as $\tau \downarrow 0$,

$$\begin{aligned} D_{\text{SRFE}}^\tau(P\|Q) &= D_{\text{KL}}(Q\|P) \\ &\quad + \tau \left(D_{\text{KL}}(Q\|P) - \frac{1}{2} \text{Var}_Q[\Delta] \right) + O(\tau^2). \end{aligned} \quad (11)$$

Proof. Define $Z(\tau)$ and $F(\tau)$ as in Section B.8. A second-order Taylor expansion of F at $\tau = 0$ gives

$$F(\tau) = F(0) + \tau F'(0) + \frac{1}{2} \tau^2 F''(0) + O(\tau^3). \quad (44)$$

Using Equations (42) and (43), we get that at $\tau = 0$, $Z(0) = \int q(x) dx = 1$, and

$$\begin{aligned} F(0) &= \log Z(0) = 0, \\ F'(0) &= Z'(0) = \int q(x) \Delta(x) dx = \int q(x) \log \frac{p(x)}{q(x)} = -D_{\text{KL}}(Q\|P), \\ F''(0) &= Z''(0) - Z'(0)^2 \\ &= \int q(x) \Delta(x)^2 dx - \left(\int q(x) \Delta(x) \right)^2 \\ &= \text{Var}_q[\Delta] \end{aligned}$$

Substituting into Equation (44) gives

$$F(\tau) = -\tau D_{\text{KL}}(Q\|P) + \frac{\tau^2}{2} \text{Var}_q[\Delta] + O(\tau^3).$$

Factoring out τ , we get

$$F(\tau) = \tau \left(-D_{\text{KL}}(Q\|P) + \frac{\tau}{2} \text{Var}_q[\Delta] + O(\tau^2) \right).$$

Then,

$$\begin{aligned} D_{\text{SRFE}}^\tau(P\|Q) &= -\frac{F(\tau)}{\tau(1-\tau)} \\ &= -\frac{\tau}{\tau(1-\tau)} \left(-D_{\text{KL}}(Q\|P) + \frac{\tau}{2} \text{Var}_q[\Delta] + O(\tau^2) \right) \\ &= \frac{1}{1-\tau} \left(D_{\text{KL}}(Q\|P) - \frac{\tau}{2} \text{Var}_q[\Delta] + O(\tau^2) \right) \end{aligned}$$

Now expand $1/(1-\tau)$ around $\tau = 0$:

$$\frac{1}{1-\tau} = 1 + \tau + O(\tau^2).$$

Thus

$$\begin{aligned} D_{\text{SRFE}}^\tau(P\|Q) &= \left(1 + \tau + O(\tau^2) \right) \left(D_{\text{KL}}(Q\|P) - \frac{\tau}{2} \text{Var}_q[\Delta] + O(\tau^2) \right) \\ &= D_{\text{KL}}(Q\|P) + \tau \left(D_{\text{KL}}(Q\|P) - \frac{1}{2} \text{Var}_q[\Delta] \right) + O(\tau^2), \end{aligned}$$

which is exactly Eq. (11). □

B.10 PROOF OF LEMMA 3.9

Lemma 3.9 (SRFE gradient). For $\tau \in (0, 1)$,

$$\nabla_\theta D_{\text{SRFE}}^\tau(P\|Q_\theta) = -\frac{1}{\tau} \mathbb{E}_{x \sim r_\tau} [\nabla_\theta \log q_\theta(x)], \quad (12)$$

where

$$r_\tau(x) := \frac{p(x)^\tau q_\theta(x)^{1-\tau}}{F(\tau)}. \quad (13)$$

Proof. Using $\nabla \log x = (\nabla x)/x$ and $D_{\text{SRFE}}^\tau(P\|Q_\theta) = -\frac{1}{\tau(1-\tau)} \log F(\tau)$,

$$\nabla_\theta D_{\text{SRFE}}^\tau(P\|Q_\theta) = -\frac{1}{\tau(1-\tau)} \frac{\nabla_\theta F(\tau)}{F(\tau)}.$$

Next,

$$\begin{aligned} \nabla_\theta F(\tau) &= \nabla_\theta \int_{\mathcal{X}} p(x)^\tau q_\theta(x)^{1-\tau} d\mu(x) \\ &= \int_{\mathcal{X}} p(x)^\tau \nabla_\theta [q_\theta(x)^{1-\tau}] d\mu(x) \\ &= \int_{\mathcal{X}} p(x)^\tau (1-\tau) q_\theta(x)^{-\tau} \nabla_\theta q_\theta(x) d\mu(x). \end{aligned}$$

Substituting in $\nabla x = x \cdot \nabla \log x$,

$$\begin{aligned}\nabla_{\theta} F(\tau) &= \int_{\mathcal{X}} p(x)^{\tau} (1-\tau) q_{\theta}(x)^{-\tau} \cdot q_{\theta}(x) \nabla_{\theta} \log q_{\theta}(x) d\mu(x) \\ &= (1-\tau) \int_{\mathcal{X}} p(x)^{\tau} q_{\theta}(x)^{1-\tau} \nabla_{\theta} \log q_{\theta}(x) d\mu(x).\end{aligned}\tag{45}$$

Substituting into $\nabla_{\theta} D_{\text{SRFE}}^{\tau}(P\|Q_{\theta})$,

$$\nabla_{\theta} D_{\text{SRFE}}^{\tau}(P\|Q_{\theta}) = -\frac{1}{\tau} \int_{\mathcal{X}} \frac{p(x)^{\tau} q_{\theta}(x)^{1-\tau}}{F(\tau)} \nabla_{\theta} \log q_{\theta}(x) d\mu(x) = -\frac{1}{\tau} \mathbb{E}_{x \sim r_{\tau}} [\nabla_{\theta} \log q_{\theta}(x)].$$

□

B.11 PROOF OF LEMMA 3.10

Lemma 3.10 (Associated CR gradient). *For $\tau \in (0, 1)$ and $u(x) = p(x)/q_{\theta}(x)$,*

$$\nabla_{\theta} D_{\text{CR}}^{\tau}(P\|Q_{\theta}) = -\frac{1}{\tau} \mathbb{E}_{x \sim Q_{\theta}} [u(x)^{\tau} \nabla_{\theta} \log q_{\theta}(x)].\tag{14}$$

Equivalently (baseline-subtracted form),

$$\nabla_{\theta} D_{\text{CR}}^{\tau}(P\|Q_{\theta}) = -\frac{1}{\tau} \mathbb{E}_{x \sim Q_{\theta}} [(u(x)^{\tau} - 1) \nabla_{\theta} \log q_{\theta}(x)].\tag{15}$$

Proof. By definition, $D_{\text{CR}}^{\tau}(P\|Q_{\theta}) = \frac{1 - F(\tau)}{\tau(1 - \tau)}$, hence

$$\nabla_{\theta} D_{\text{CR}}^{\tau}(P\|Q_{\theta}) = -\frac{1}{\tau(1 - \tau)} \nabla_{\theta} F(\tau).$$

Substituting in Eq. (45) and simplifying,

$$\nabla_{\theta} D_{\text{CR}}^{\tau}(P\|Q_{\theta}) = -\frac{1}{\tau} \int_{\mathcal{X}} p(x)^{\tau} q_{\theta}(x)^{1-\tau} \nabla_{\theta} \log q_{\theta}(x) d\mu(x).$$

Since $p(x)^{\tau} q_{\theta}(x)^{1-\tau} = q_{\theta}(x) \left(\frac{p(x)}{q_{\theta}(x)}\right)^{\tau} = q_{\theta}(x) u(x)^{\tau}$, we obtain

$$\nabla_{\theta} D_{\text{CR}}^{\tau}(P\|Q_{\theta}) = -\frac{1}{\tau} \int_{\mathcal{X}} q_{\theta}(x) u(x)^{\tau} \nabla_{\theta} \log q_{\theta}(x) d\mu(x) = -\frac{1}{\tau} \mathbb{E}_{x \sim Q_{\theta}} [u(x)^{\tau} \nabla_{\theta} \log q_{\theta}(x)],$$

which is Eq. (14). Finally, using $\mathbb{E}_{x \sim Q_{\theta}} [\nabla_{\theta} \log q_{\theta}(x)] = \nabla_{\theta} \int q_{\theta}(x) d\mu(x) = \nabla_{\theta} 1 = 0$, we can subtract the constant baseline 1 to get the equivalent form with $(u^{\tau} - 1)$ as in Eq. (15). □

B.12 PROOF OF LEMMA 3.11

Lemma 3.11 (Associated CR gradient estimator and second-moment bound). *Let q_{θ} be a smooth density model and assume $\|\nabla_{\theta} \log q_{\theta}(x)\|^2 \leq C$ for all x . Fix $\tau \in (0, 1)$ and define $u(x) = p(x)/q_{\theta}(x)$. The unbiased one-sample stochastic gradient estimator for the associated CR under $X \sim Q_{\theta}$ is*

$$g_{\text{CR}}(X) := -\frac{1}{\tau} u(X)^{\tau} \nabla_{\theta} \log q_{\theta}(X).\tag{16}$$

Moreover,

$$\mathbb{E}_{X \sim Q_\theta} [\|g_{\text{CR}}(X)\|^2] \leq \frac{C}{\tau^2} \int_{\mathcal{X}} q_\theta(x) u(x)^{2\tau} d\mu(x), \quad (17)$$

which diverges whenever $q_\theta(x) \rightarrow 0$ on sets where $p(x) > 0$ and the integral is infinite.

The variance of the expectation of the gradient is trivially zero; however, we consider the variance of the stochastic gradient for insight into the learning dynamics of each objective.

Proof. From Eq. (14), define the stochastic gradient of CR as $g_{\text{CR}}(x) = -(1/\tau)u(x)^\tau \nabla_\theta \log q_\theta(x)$ for $x \sim Q_\theta$ and assume $\|\nabla_\theta \log q_\theta(x)\|^2 \leq C$.

$$\|g_{\text{CR}}(x)\|^2 = \frac{1}{\tau^2} u(x)^{2\tau} \|\nabla_\theta \log q_\theta(x)\|^2 \leq \frac{C}{\tau^2} u(x)^{2\tau}.$$

The identity $\mathbb{E}_{Q_\theta}[u^{2\tau}] = \int q_\theta u^{2\tau} d\mu$ is immediate. Therefore

$$\mathbb{E}_{x \sim Q_\theta} [\|g_{\text{CR}}(x)\|^2] \leq \frac{C}{\tau^2} \int q_\theta(x) u(x)^{2\tau} d\mu(x),$$

which gives us Eq. (17). □

B.13 PROOF OF LEMMA 3.12

Lemma 3.12 (SRFE gradient estimators and second-moment bounds). *Let q_θ be differentiable in θ and assume differentiation can be interchanged with integration. Fix $\tau \in (0, 1)$ and assume $\|\nabla_\theta \log q_\theta(x)\|^2 \leq C$ for all x . Define $F(\tau) = \int_{\mathcal{X}} p(x)^\tau q_\theta(x)^{1-\tau} d\mu(x)$, $r_\tau(x) = \frac{p(x)^\tau q_\theta(x)^{1-\tau}}{F(\tau)}$, and $u(x) = p(x)/q_\theta(x)$.*

(i) *Escort-sampling estimator.* If $X \sim r_\tau$, define

$$g_{\text{SRFE}}^{(r)}(X) := -\frac{1}{\tau} \nabla_\theta \log q_\theta(X). \quad (18)$$

Then $g_{\text{SRFE}}^{(r)}$ is unbiased for $\nabla_\theta D_{\text{SRFE}}^\tau(P\|Q_\theta)$ and satisfies

$$\mathbb{E}_{X \sim r_\tau} [\|g_{\text{SRFE}}^{(r)}(X)\|^2] \leq \frac{C}{\tau^2}. \quad (19)$$

(ii) *Q_θ -sampling (importance-weighted) estimator.* If $X \sim Q_\theta$, define

$$g_{\text{SRFE}}^{(q)}(X) := -\frac{1}{\tau} \frac{u(X)^\tau}{F(\tau)} \nabla_\theta \log q_\theta(X). \quad (20)$$

Then $g_{\text{SRFE}}^{(q)}$ is unbiased for $\nabla_\theta D_{\text{SRFE}}^\tau(P\|Q_\theta)$ and satisfies

$$\mathbb{E}_{X \sim Q_\theta} [\|g_{\text{SRFE}}^{(q)}(X)\|^2] \leq \frac{C}{\tau^2 F(\tau)^2} \int_{\mathcal{X}} q_\theta(x) u(x)^{2\tau} d\mu(x). \quad (21)$$

Proof. We use the SRFE gradient identity (proved in Lemma 3.9):

$$\nabla_\theta D_{\text{SRFE}}^\tau(P\|Q_\theta) = -\frac{1}{\tau} \mathbb{E}_{X \sim r_\tau} [\nabla_\theta \log q_\theta(X)], \quad r_\tau(x) = \frac{p(x)^\tau q_\theta(x)^{1-\tau}}{F(\tau)}. \quad (46)$$

(i) **Unbiasedness under escort sampling.** By definition from Eq. (18),

$$\mathbb{E}_{X \sim r_\tau} [g_{\text{SRFE}}^{(r)}(X)] = -\frac{1}{\tau} \mathbb{E}_{X \sim r_\tau} [\nabla_\theta \log q_\theta(X)] = \nabla_\theta D_{\text{SRFE}}^\tau(P\|Q_\theta),$$

which proves unbiasedness.

(i) Second moment bound. Using $\|g_{\text{SRFE}}^{(r)}(X)\|^2 = (1/\tau^2)\|\nabla_\theta \log q_\theta(X)\|^2$ and the uniform bound $\|\nabla_\theta \log q_\theta(x)\|^2 \leq C$,

$$\mathbb{E}_{X \sim r_\tau}[\|g_{\text{SRFE}}^{(r)}(X)\|^2] = \frac{1}{\tau^2} \mathbb{E}_{X \sim r_\tau}[\|\nabla_\theta \log q_\theta(X)\|^2] \leq \frac{C}{\tau^2},$$

which is Eq. (19).

(ii) Unbiasedness under Q_θ -sampling (importance form). First note that for any integrable test function φ ,

$$\mathbb{E}_{X \sim r_\tau}[\varphi(X)] = \int_{\mathcal{X}} r_\tau(x) \varphi(x) d\mu(x) = \frac{1}{F(\tau)} \int_{\mathcal{X}} p(x)^\tau q_\theta(x)^{1-\tau} \varphi(x) d\mu(x).$$

Since $p(x)^\tau q_\theta(x)^{1-\tau} = q_\theta(x) \left(\frac{p(x)}{q_\theta(x)}\right)^\tau = q_\theta(x) u(x)^\tau$, this becomes

$$\mathbb{E}_{X \sim r_\tau}[\varphi(X)] = \frac{1}{F(\tau)} \int_{\mathcal{X}} q_\theta(x) u(x)^\tau \varphi(x) d\mu(x) = \frac{1}{F(\tau)} \mathbb{E}_{X \sim Q_\theta}[u(X)^\tau \varphi(X)]. \quad (47)$$

Apply Eq. (47) with $\varphi(X) = \nabla_\theta \log q_\theta(X)$ to get

$$\mathbb{E}_{X \sim r_\tau}[\nabla_\theta \log q_\theta(X)] = \frac{1}{F(\tau)} \mathbb{E}_{X \sim Q_\theta}[u(X)^\tau \nabla_\theta \log q_\theta(X)], \quad (48)$$

and substitute into Eq. (46):

$$\nabla_\theta D_{\text{SRFE}}^\tau(P\|Q_\theta) = -\frac{1}{\tau} \cdot \frac{1}{F(\tau)} \mathbb{E}_{X \sim Q_\theta}[u(X)^\tau \nabla_\theta \log q_\theta(X)] = \mathbb{E}_{X \sim Q_\theta}[g_{\text{SRFE}}^{(q)}(X)],$$

which proves unbiasedness of Eq. (20).

(ii) Second moment bound. By Eq. (20) and the uniform score bound,

$$\|g_{\text{SRFE}}^{(q)}(X)\|^2 = \frac{1}{\tau^2 F(\tau)^2} u(X)^{2\tau} \|\nabla_\theta \log q_\theta(X)\|^2 \leq \frac{C}{\tau^2 F(\tau)^2} u(X)^{2\tau}.$$

Taking expectations under $X \sim Q_\theta$ yields

$$\mathbb{E}_{X \sim Q_\theta}[\|g_{\text{SRFE}}^{(q)}(X)\|^2] \leq \frac{C}{\tau^2 F(\tau)^2} \mathbb{E}_{X \sim Q_\theta}[u(X)^{2\tau}].$$

Finally,

$$\mathbb{E}_{X \sim Q_\theta}[u(X)^{2\tau}] = \int_{\mathcal{X}} q_\theta(x) u(x)^{2\tau} d\mu(x),$$

which gives Eq. (21). □

B.14 PROOF OF THEOREM 3.13

Theorem 3.13 (Variational characterization of SRFE (information-geometric form)).

$$D_{\text{SRFE}}^\tau(P\|Q) = \min_{r \in \mathcal{P}(\mathcal{X})} \left\{ \frac{1}{\tau} D_{\text{KL}}(r\|Q) + \frac{1}{1-\tau} D_{\text{KL}}(r\|P) \right\}, \quad (22)$$

and the unique minimizer is the escort (Chernoff) distribution

$$r_\tau(x) = \frac{p(x)^\tau q(x)^{1-\tau}}{\int_{\mathcal{X}} p(u)^\tau q(u)^{1-\tau} d\mu(u)}. \quad (23)$$

Equivalently, the objective in Eq. (22) admits the decomposition

$$\frac{1}{\tau(1-\tau)} D_{\text{KL}}(r \| r_\tau) + D_{\text{SRFE}}^\tau(P \| Q), \quad (24)$$

which exhibits an information-geometric (Pythagorean) relation with projection onto the τ -escort path.

Proof. Fix $\tau \in (0, 1)$ and define

$$Z_\tau := \int_{\mathcal{X}} p(x)^\tau q(x)^{1-\tau} d\mu(x) \in (0, \infty), \quad r_\tau(x) := \frac{p(x)^\tau q(x)^{1-\tau}}{Z_\tau}.$$

For any $r \in \mathcal{P}(\mathcal{X})$ with $r \ll p$ and $r \ll q$, expand the KL terms:

$$D_{\text{KL}}(r \| q) = \int r \log \frac{r}{q} d\mu, \quad D_{\text{KL}}(r \| p) = \int r \log \frac{r}{p} d\mu.$$

Consider the functional

$$J(r) := \frac{1}{\tau} D_{\text{KL}}(r \| q) + \frac{1}{1-\tau} D_{\text{KL}}(r \| p).$$

Combine the two integrals:

$$\begin{aligned} J(r) &= \int r \left[\frac{1}{\tau} \log \frac{r}{q} + \frac{1}{1-\tau} \log \frac{r}{p} \right] d\mu \\ &= \int r \left[\left(\frac{1}{\tau} + \frac{1}{1-\tau} \right) \log r - \frac{1}{\tau} \log q - \frac{1}{1-\tau} \log p \right] d\mu \\ &= \frac{1}{\tau(1-\tau)} \int r [\log r - \tau \log p - (1-\tau) \log q] d\mu \\ &= \frac{1}{\tau(1-\tau)} \int r \log \frac{r}{p^\tau q^{1-\tau}} d\mu. \end{aligned}$$

Using $p^\tau q^{1-\tau} = Z_\tau r_\tau$, we obtain

$$\begin{aligned} \int r \log \frac{r}{p^\tau q^{1-\tau}} d\mu &= \int r \log \frac{r}{Z_\tau r_\tau} d\mu \\ &= \int r \left[\log \frac{r}{r_\tau} - \log Z_\tau \right] d\mu \\ &= \int r \log \frac{r}{r_\tau} d\mu - \log Z_\tau \int r d\mu \\ &= \int r \log \frac{r}{r_\tau} d\mu - \log Z_\tau \\ &= D_{\text{KL}}(r \| r_\tau) - \log Z_\tau. \end{aligned}$$

Therefore,

$$J(r) = \frac{1}{\tau(1-\tau)} D_{\text{KL}}(r \| r_\tau) - \frac{1}{\tau(1-\tau)} \log Z_\tau. \quad (49)$$

By nonnegativity of KL divergence, $D_{\text{KL}}(r \| r_\tau) \geq 0$ with equality iff $r = r_\tau$ a.e. Hence, $J(r)$ is minimized uniquely at r_τ and

$$\min_r J(r) = -\frac{1}{\tau(1-\tau)} \log Z_\tau.$$

Comparing with Eq. (4) yields Eq. (22) and the minimizer Eq. (23).

Finally, rearranging Eq. (49) gives the Pythagorean decomposition Eq. (24). \square

B.15 PROOF OF THEOREM 3.14

Theorem 3.14 (Riemannian metric induced by SRFE equals Fisher-Rao). *Let $\{p_\theta : \theta \in \Theta \subset \mathbb{R}^d\}$ be a smooth statistical model on $(\mathcal{X}, \Sigma, \mu)$ with strictly positive densities. Fix $\tau \in (0, 1)$ and define the SRFE divergence*

$$D_{\text{SRFE}}^\tau(p_\theta \| p_{\theta'}) := -\frac{1}{\tau(1-\tau)} \log \int_{\mathcal{X}} p_\theta(x)^\tau p_{\theta'}(x)^{1-\tau} d\mu(x). \quad (25)$$

Assume the usual regularity conditions allowing differentiation under the integral sign and the identities

$$\mathbb{E}_\theta[\partial_i \log p_\theta] = 0, \quad \mathbb{E}_\theta[\partial_{ij} \log p_\theta] = -I_{ij}(\theta),$$

where $I(\theta)$ is the Fisher information matrix

$$I_{ij}(\theta) := \mathbb{E}_\theta[\partial_i \log p_\theta(X) \partial_j \log p_\theta(X)].$$

Then the second-order expansion around $\theta' = \theta$ is

$$D_\tau^{\text{SRFE}}(p_\theta \| p_{\theta+\delta}) = \frac{1}{2} \delta^\top I(\theta) \delta + O(\|\delta\|^3). \quad (26)$$

Consequently, the Riemannian metric induced by SRFE,

$$g_{ij}^{(\text{SRFE})}(\theta) := \left. \frac{\partial^2}{\partial \theta^i \partial \theta^j} D_\tau^{\text{SRFE}}(p_\theta \| p_{\theta'}) \right|_{\theta'=\theta},$$

coincides with the Fisher-Rao metric:

$$g_{ij}^{(\text{SRFE})}(\theta) = I_{ij}(\theta). \quad (27)$$

Proof. Fix θ and write $\ell_\theta(x) := \log p_\theta(x)$. Let $\theta' = \theta + \delta$ with $\delta \in \mathbb{R}^d$ small, and define

$$A(\delta) := \int p_\theta(x)^\tau p_{\theta+\delta}(x)^{1-\tau} d\mu(x).$$

Since $p_{\theta+\delta} = p_\theta \exp(\ell_{\theta+\delta} - \ell_\theta)$, we get

$$\begin{aligned} A(\delta) &= \int p_\theta(x)^\tau (p_\theta(x) \exp[\ell_{\theta+\delta}(x) - \ell_\theta(x)])^{1-\tau} d\mu(x) \\ &= \int p_\theta(x)^\tau p_\theta(x)^{1-\tau} \exp[\ell_{\theta+\delta}(x) - \ell_\theta(x)]^{1-\tau} d\mu(x) \\ &= \int p_\theta(x) \exp((1-\tau)[\ell_{\theta+\delta}(x) - \ell_\theta(x)]) d\mu(x) \\ &= \mathbb{E}_\theta[\exp((1-\tau)\Delta_\ell(X))], \end{aligned}$$

where $\Delta_\ell(x) := \ell_{\theta+\delta}(x) - \ell_\theta(x)$.

By a second-order Taylor expansion of $\ell_{\theta+\delta}$ around θ ,

$$\Delta_\ell(x) = \delta^\top s_\theta(x) + \frac{1}{2} \delta^\top H_\theta(x) \delta + O(\|\delta\|^3),$$

where $s_\theta(x) := \nabla_\theta \ell_\theta(x)$ is the score and $H_\theta(x) := \nabla_\theta^2 \ell_\theta(x)$ is the Hessian. Hence

$$(1-\tau)\Delta_\ell(x) = (1-\tau) \delta^\top s_\theta(x) + \frac{1-\tau}{2} \delta^\top H_\theta(x) \delta + O(\|\delta\|^3).$$

We now expand $\log A(\delta) = \log \mathbb{E}_\theta[\exp((1-\tau)\Delta_\ell(X))]$ to second order in δ . Let

$$U(x) := \delta^\top s_\theta(x), \quad V(x) := \frac{1}{2} \delta^\top H_\theta(x) \delta.$$

Then $(1 - \tau)\Delta_\ell = (1 - \tau)U + (1 - \tau)V + O(\|\delta\|^3)$, where $U = O(\|\delta\|)$ and $V = O(\|\delta\|^2)$. Using the standard cumulant expansion

$$\log \mathbb{E}[e^{aU+bV}] = a \mathbb{E}[U] + b \mathbb{E}[V] + \frac{a^2}{2} \text{Var}(U) + O(\|\delta\|^3),$$

where $\text{Var}(V) = O(\|\delta\|^4)$, as $V = O(\|\delta\|^2)$, is absorbed into $O(\|\delta\|^3)$, we obtain

$$\log A(\delta) = (1 - \tau)\mathbb{E}_\theta[V] + \frac{(1 - \tau)^2}{2} \text{Var}_\theta(U) + O(\|\delta\|^3).$$

Now, we can compute each term. First, by regularity, $\mathbb{E}_\theta[s_\theta] = 0$, hence $\mathbb{E}_\theta[U] = \delta^\top \mathbb{E}_\theta[s_\theta] = 0$ (so there is no linear term). Next,

$$\text{Var}_\theta(U) = \mathbb{E}_\theta[U^2] = \mathbb{E}_\theta[(\delta^\top s_\theta)^2] = \delta^\top I(\theta) \delta.$$

Finally,

$$\mathbb{E}_\theta[V] = \frac{1}{2} \delta^\top \mathbb{E}_\theta[H_\theta(X)] \delta = -\frac{1}{2} \delta^\top I(\theta) \delta,$$

using $\mathbb{E}_\theta[\partial_{ij} \ell_\theta] = -I_{ij}(\theta)$.

Substituting into Section B.15 gives

$$\log A(\delta) = (1 - \tau) \left(-\frac{1}{2} \delta^\top I(\theta) \delta \right) + \frac{(1 - \tau)^2}{2} (\delta^\top I(\theta) \delta) + O(\|\delta\|^3).$$

Factor the quadratic form:

$$\log A(\delta) = -\frac{\tau(1 - \tau)}{2} \delta^\top I(\theta) \delta + O(\|\delta\|^3).$$

By definition Eq. (25),

$$D_\tau^{\text{SRFE}}(p_\theta \| p_{\theta+\delta}) = -\frac{1}{\tau(1 - \tau)} \log A(\delta) = \frac{1}{2} \delta^\top I(\theta) \delta + O(\|\delta\|^3),$$

which proves Eq. (26). Differentiating twice with respect to θ' at $\theta' = \theta$ yields the induced metric $g_{ij}^{(\text{SRFE})}(\theta) = I_{ij}(\theta)$, proving Eq. (27). \square

B.16 PROOF OF THEOREM 3.16

Theorem 3.16 (SRFE controls large deviations of excess codelength). *Let $(\mathcal{X}, \Sigma, \mu)$ be a measurable space and let $P, Q \ll \mu$ with densities p, q . Fix $\tau \in (0, 1)$ and assume $F(\tau) = \int p(x)^\tau q(x)^{1-\tau} d\mu(x) \in (0, \infty)$. Then for any $a \in \mathbb{R}$,*

$$\Pr_{X \sim Q} [\Delta(X) \geq a] \leq \exp\left(-\tau a - \tau(1 - \tau) D_{\text{SRFE}}^\tau(P \| Q)\right). \quad (28)$$

Proof. For $\tau \in (0, 1)$, Markov's inequality yields

$$\Pr_q(\Delta \geq a) = \Pr_q(e^{\tau\Delta} \geq e^{\tau a}) \leq e^{-\tau a} \mathbb{E}_q[e^{\tau\Delta}].$$

Since $e^{\tau\Delta} = e^{\tau \log p/q} = (p/q)^\tau$, we have

$$\mathbb{E}_q[e^{\tau\Delta}] = \int q(x) \left(\frac{p(x)}{q(x)}\right)^\tau dx$$

Rearranging SRFE,

$$\begin{aligned} D_{\text{SRFE}}^\tau(P \| Q) &= -\frac{1}{\tau(1 - \tau)} \log \int q(x) \left(\frac{p(x)}{q(x)}\right)^\tau dx \\ \exp(-\tau(1 - \tau)) D_{\text{SRFE}}^\tau(P \| Q) &= \int q(x) \left(\frac{p(x)}{q(x)}\right)^\tau dx \end{aligned}$$

Substituting this into the Markov bound gives

$$\begin{aligned} \Pr_q(\Delta \geq a) &\leq \exp(-\tau a) \exp(-\tau(1-\tau)) D_{\text{SRFE}}^\tau(P\|Q) \\ &= \exp(-\tau a - \tau(1-\tau)) D_{\text{SRFE}}^\tau(P\|Q), \end{aligned}$$

which matches Eq. (28). □

B.17 PROOF OF THEOREM 3.17

Theorem 3.17 (Gibbs variational characterization of SRFE). *For fixed $\tau \in (0, 1)$ and $r \in \mathcal{P}(\mathcal{X})$*

$$D_{\text{SRFE}}^\tau(P\|Q) = \min_r \left\{ \frac{1}{\tau} D_{\text{KL}}(r\|Q) + \frac{1}{1-\tau} D_{\text{KL}}(r\|P) \right\}, \quad (29)$$

with a unique minimizer $r_\tau(x)$.

Proof. Consider the functional $J(r) := \frac{1}{\tau} D_{\text{KL}}(r\|P) + \frac{1}{1-\tau} D_{\text{KL}}(r\|Q)$ over densities r with $\int r = 1$. Writing out the KL divergences and collecting terms gives

$$J(r) = \int r \log r - \int r (\tau \log p + (1-\tau) \log q) + \text{const}(\tau, p, q).$$

By the Gibbs (log-sum) variational principle, the minimizer satisfies $\log r = \tau \log p + (1-\tau) \log q - \log Z + \text{const}$, hence $r = r_\tau$. Substituting r_τ back into $J(r)$ yields $J(r_\tau) = -\frac{1}{\tau(1-\tau)} \log \int p^\tau q^{1-\tau} = D_{\text{SRFE}}^\tau(P\|Q)$. □

B.18 PROOF OF COROLLARY 3.18

Corollary 3.18 (KL upper bounds for SRFE).

$$D_{\text{SRFE}}^\tau(P\|Q) \leq \frac{1}{1-\tau} D_{\text{KL}}(P\|Q), \quad (30)$$

$$D_{\text{SRFE}}^\tau(P\|Q) \leq \frac{1}{\tau} D_{\text{KL}}(Q\|P). \quad (31)$$

Equivalently,

$$D_{\text{SRFE}}^\tau(P\|Q) \leq \min \left\{ \frac{1}{1-\tau} D_{\text{KL}}(P\|Q), \frac{1}{\tau} D_{\text{KL}}(Q\|P) \right\}.$$

Proof. Using the variational characterization of SRFE, define

$$J(r) := \frac{1}{\tau} D_{\text{KL}}(r\|P) + \frac{1}{1-\tau} D_{\text{KL}}(r\|Q), \quad r \in \mathcal{P}(\mathcal{X}).$$

Then $D_{\text{SRFE}}^\tau(P\|Q) = \min_r J(r)$, so for any admissible r we have $D_{\text{SRFE}}^\tau(P\|Q) \leq J(r)$.

Choosing $r = P$ gives

$$J(P) = \frac{1}{\tau} D_{\text{KL}}(P\|P) + \frac{1}{1-\tau} D_{\text{KL}}(P\|Q) = \frac{1}{1-\tau} D_{\text{KL}}(P\|Q),$$

and choosing $r = Q$ gives

$$J(Q) = \frac{1}{\tau} D_{\text{KL}}(Q\|P) + \frac{1}{1-\tau} D_{\text{KL}}(Q\|Q) = \frac{1}{\tau} D_{\text{KL}}(Q\|P).$$

Taking the minimum of these two upper bounds yields the stated result. □

Why SRFE is upper bounded by scaled KL endpoints The variational form

$$D_{\text{SRFE}}^\tau(P\|Q) = \min_{r \in \mathcal{P}(\mathcal{X})} \left\{ \frac{1}{\tau} D_{\text{KL}}(r\|P) + \frac{1}{1-\tau} D_{\text{KL}}(r\|Q) \right\}$$

shows that SRFE is the *best* achievable weighted compromise between proximity to P and proximity to Q in KL geometry. Evaluating this objective at the two extreme choices $r = P$ and $r = Q$ yields feasible (not necessarily optimal) values

$$J(P) = \frac{1}{1-\tau} D_{\text{KL}}(P\|Q), \quad J(Q) = \frac{1}{\tau} D_{\text{KL}}(Q\|P),$$

and since a minimum is never larger than any feasible value, we obtain the endpoint bounds

$$D_{\text{SRFE}}^\tau(P\|Q) \leq \min \left\{ \frac{1}{1-\tau} D_{\text{KL}}(P\|Q), \frac{1}{\tau} D_{\text{KL}}(Q\|P) \right\}.$$

Thus, SRFE cannot exceed the scaled forward or reverse KL costs of moving directly to either endpoint; instead it selects an intermediate escort distribution that improves upon both whenever possible.

B.19 PROOF OF COROLLARY 3.19

Corollary 3.19 (MDL interpretation: exponential tail control). Let $\Delta(x) = \log \frac{p(x)}{q(x)}$. For any $a \in \mathbb{R}$,

$$\Pr_{X \sim Q} [\Delta(X) \geq a] \leq \exp \left(-\tau a - \tau(1-\tau) D_{\text{SRFE}}^\tau(P\|Q) \right). \quad (32)$$

Proof. By definition, $\text{Excess}(X) = \log \frac{p(X)}{q(X)}$, so

$$\Pr_{X \sim Q} [\text{Excess}(X) \geq a] = \Pr_{X \sim Q} \left[\log \frac{p(X)}{q(X)} \geq a \right].$$

Applying Theorem 3.16 with $\Delta(X) = \log \frac{p(X)}{q(X)}$ yields Eq. (32). □

C ADDITIONAL FIGURES

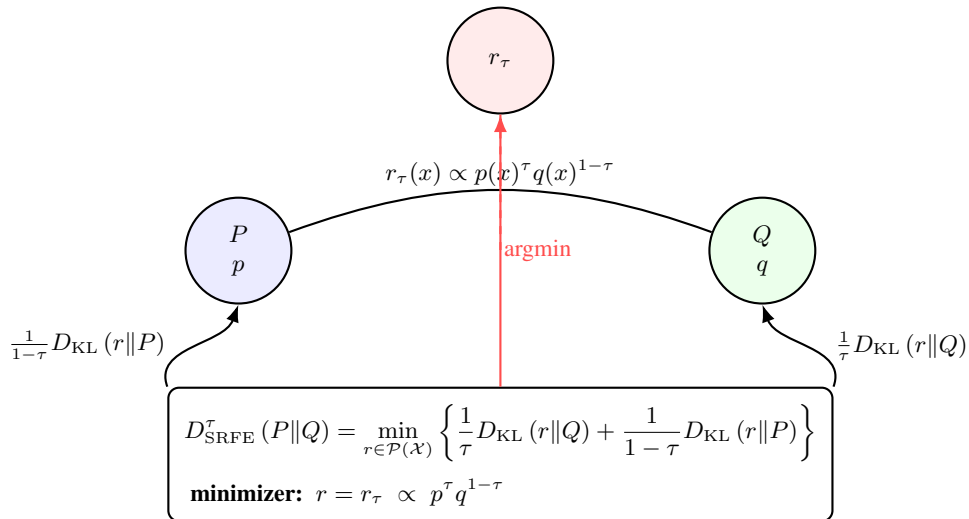


Figure 7: SRFE as a KL-regularized variational projection onto the escort (Chernoff) distribution r_τ .

D TRAINING METHOD

The goal of training is to align a single Gaussian model q_θ representing a predicted probability distribution to a mixture of three Gaussians representing the true distribution p . Training consists of sampling from either q_θ or the mixture of Gaussians (depending on the objective function used) to compute a loss value to apply gradient descent onto. Algorithm 1 presents our implementation of SRFE for training, while Algorithm 2 presents both the actual training algorithm and implementations of forward KL and reverse KL.

Algorithm 1 calculates a loss by sampling n samples from q_θ via reparameterization before computing the log probabilities of the samples in both q_θ and p and then calculating the log importance ratios between the two probabilities for each sample. The average of the log importance ratios multiplied by τ and raised to the power of e becomes $F(\tau)$, which is used to calculate the loss $\mathcal{L}_{\text{SRFE}} = -\frac{\log F(\tau)}{\tau(1-\tau)}$. Importantly, the maximum log importance ratio is summed out for numerical stability, and a clamp is used to keep $F(\tau)$ between 10^{-10} and 1.0 to prevent negative/undefined losses.

Algorithm 1: Compute SRFE Loss

Input: Variational distribution q_θ , Target distribution p , Parameter $\tau \in (0, 1)$, Samples n

Output: SRFE loss $\mathcal{L}_{\text{SRFE}}$

```

1 Sample  $\{x_i\}_{i=1}^n \sim q_\theta$  via reparameterization;
2 for  $i = 1$  to  $n$  do
3    $\ell_q^{(i)} \leftarrow \log q_\theta(x_i)$ ;
4    $\ell_p^{(i)} \leftarrow \log p(x_i)$ ;
5    $r^{(i)} \leftarrow \ell_p^{(i)} - \ell_q^{(i)}$ ; // Log importance ratio
6  $r_{\max} \leftarrow \max_i r^{(i)}$ ; // For numerical stability
7  $F(\tau) \leftarrow \frac{1}{n} \sum_{i=1}^n \exp(\tau \cdot (r^{(i)} - r_{\max}))$ ;
8  $F(\tau) \leftarrow F(\tau) \cdot \exp(\tau \cdot r_{\max})$ ; // Restore scale
9  $F(\tau) \leftarrow \text{clamp}(F(\tau), 10^{-10}, 1.0)$ ; // Enforce  $F(\tau) \leq 1$ 
10  $\mathcal{L}_{\text{SRFE}} \leftarrow -\frac{\log F(\tau)}{\tau(1-\tau)}$ ;
11 return  $\mathcal{L}_{\text{SRFE}}$ 

```

Algorithm 2 calculates reverse KL by sampling n samples from p and calculating the average of the sample’s log importance ratios between p and q_θ . Forward KL is calculated by sampling n samples from q_θ and calculating the average of the sample’s log importance ratios between q_θ and p . Training is performed over T iterations using the Adam optimizer. q_θ is parameterized by μ and $\log \sigma$, both of which are 2-dimensional vectors that are initialized as vectors of zeros.

In each experiment, the following 4 metrics are calculated:

- Mode Coverage: The number of modes of p covered by q_θ .
- Effective Sample Size (ESS): Estimate of the number of samples needed from p to get the same precision as q_θ ; used in understanding sampling efficiency.
- Entropy Error: The absolute difference between the entropy of p and the entropy q
- Test Log-Likelihood (Test Log-Lik): The average log probability in terms of q of samples from p .

Algorithm 3 presents how these metrics are calculated.

Experiment 1 compares the forward KL and reverse KL objectives to SRFE at different τ values. Algorithm 4 connects Algorithm 2 and Algorithm 3 to gather data for these comparisons.

Experiment 2 focuses on finding the optimal τ values for a specific measure. For each τ value tested, Algorithm 5 performs M trial runs, collecting from each trial the mode coverage, effective sample size, entropy error, and test log-likelihood. The outputs are the means and standard deviations for mode coverage, effective sample size, entropy error, and test log-likelihood of each τ value.

Experiment 3 focuses on comparing fixed $\tau \in \{0.01, 0.5, 0.99\}$ against linear and stepwise schedules for τ . Algorithm 6 introduces an alteration to the training process found in Algorithm 2. This alteration allows SRFE to change its τ values by the scheduler.

Algorithm 2: Train Variational Distribution with SRFE

Input: Target distribution p , Divergence type $D \in \{\text{F-KL}, \text{R-KL}, \text{SRFE}\}$, Parameter τ , Iterations T , Learning rate α , Samples n

Output: Optimized parameters θ^* , Loss history

```
1 Initialize  $\theta \leftarrow \{\mu = 0, \log \sigma = 0\}$ ;  
2 Initialize Adam optimizer with learning rate  $\alpha$ ;  
3  $\mathcal{L}_{\text{history}} \leftarrow []$ ;  
4 for  $t = 1$  to  $T$  do  
5   if  $D = \text{SRFE}$  then  
6      $\mathcal{L} \leftarrow \text{ComputeSRFELoss}(q_\theta, p, \tau, n)$ ;  
7   else if  $D = \text{F-KL}$  then  
8     Sample  $\{x_i\}_{i=1}^n \sim q_\theta$ ;  
9      $\mathcal{L} \leftarrow \frac{1}{n} \sum_{i=1}^n [\log q_\theta(x_i) - \log p(x_i)]$ ;  
10  else  
11    Sample  $\{x_i\}_{i=1}^n \sim p$ ;  
12     $\mathcal{L} \leftarrow \frac{1}{n} \sum_{i=1}^n [\log p(x_i) - \log q_\theta(x_i)]$ ;  
13   $g \leftarrow \nabla_\theta \mathcal{L}$ ;  
14   $\theta \leftarrow \text{Adam.step}(\theta, g)$ ;  
15  Append  $\mathcal{L}$  to  $\mathcal{L}_{\text{history}}$ ;  
16 return  $\theta, \mathcal{L}_{\text{history}}$ 
```

Algorithm 3: Evaluate Approximation Quality

Input: Variational distribution q_θ , Target distribution p , Evaluation samples n_{eval}

Output: Metrics: mode coverage, ESS, entropy error, test log-likelihood

```
// Mode Coverage  
1 coverage  $\leftarrow 0$ ;  
2 for each mode  $m_j$  of  $p$  do  
3   if  $q_\theta(m_j) > 0.01 \cdot \max_k q_\theta(m_k)$  then  
4     coverage  $\leftarrow$  coverage + 1;  
  
// Effective Sample Size  
5 Sample  $\{x_i\}_{i=1}^{n_{\text{eval}}} \sim q_\theta$ ;  
6 for  $i = 1$  to  $n_{\text{eval}}$  do  
7    $w_i \leftarrow \exp(\log p(x_i) - \log q_\theta(x_i))$ ;  
8 Normalize:  $w_i \leftarrow w_i / \sum_j w_j$ ;  
9 ESS  $\leftarrow (\sum_i w_i)^2 / \sum_i w_i^2$ ;  
  
// Entropy Error  
10  $H(q) \leftarrow -\mathbb{E}_{x \sim q_\theta} [\log q_\theta(x)]$  ; // Analytical for Gaussian  
11 Sample  $\{x_i\}_{i=1}^{100000} \sim p$ ;  
12  $H(p) \leftarrow -\frac{1}{100000} \sum_{i=1}^{100000} \log p(x_i)$ ;  
13 entropy_error  $\leftarrow |H(q) - H(p)|$ ;  
// Test Log-Likelihood  
14 Sample  $\{x_i\}_{i=1}^{1000} \sim p$ ;  
15 test_ll  $\leftarrow \frac{1}{1000} \sum_{i=1}^{1000} \log q_\theta(x_i)$ ;  
16 return coverage, ESS, entropy_error, test_ll
```

Experiment 4 adds contamination to the original Gaussian mixture in the form of increased probability for samples in the range $[-10, 10]^2$. The strength of the contamination is controlled by an outlier weight value. Algorithm 7 provides pseudocode for testing SRFE with various values of τ for a given outlier weight.

Finally, Table 1 contains the specific conditions we used for running each of our experiments.

Algorithm 4: SRFE, Forward KL, and Reverse KL Comparison (Experiment 1)

Input: Target distribution p , Configurations with divergence type and tau $\{(D_k, \tau_k)\}_{k=1}^K$ **Output:** Metrics and final loss for each divergence tested

```
1 results  $\leftarrow$  [];  
2 for  $k = 1$  to  $K$  do  
3    $D \leftarrow D_k; \tau \leftarrow \tau_k;$  // Non-SRFE divergences typically have null values for  $\tau$   
4    $\theta, \mathcal{L}_{history} \leftarrow \text{TrainVIDist}(p, D, \tau, T=2000, \alpha=0.05, n=5000);$   
5   metrics  $\leftarrow \text{EvaluateApproximation}(q_\theta, p, n_{eval}=10000);$   
6   Append  $(D, \tau, \text{metrics}, \mathcal{L}_{history})$  to results;  
7 return results
```

Algorithm 5: Tau Parameter Sweep (Experiment 2)

Input: Target distribution p , Tau values $\{\tau_k\}_{k=1}^K$, Number of trials M **Output:** Mean and standard deviation of metrics for each τ

```
1 results  $\leftarrow$  [];  
2 for  $k = 1$  to  $K$  do  
3    $\tau \leftarrow \tau_k;$   
4   trial_metrics  $\leftarrow$  [];  
5   for  $m = 1$  to  $M$  do  
6      $\theta, _ \leftarrow \text{TrainVIDist}(p, \text{SRFE}, \tau, T=2000, \alpha=0.05, n=5000);$   
7     metrics  $\leftarrow \text{EvaluateApproximation}(q_\theta, p, n_{eval}=10000);$   
8     Append metrics to trial_metrics;  
   // Aggregate across trials  
9   for each metric  $\in \{\text{coverage}, \text{ESS}, \text{entropy\_error}, \text{test\_ll}\}$  do  
10     $\mu_{\text{metric}} \leftarrow \text{mean}(\text{trial\_metrics}[\text{metric}]);$   
11     $\sigma_{\text{metric}} \leftarrow \text{std}(\text{trial\_metrics}[\text{metric}]);$   
12    Append  $(\tau, \mu_{\text{metric}}, \sigma_{\text{metric}})$  to results;  
13 return results
```

Algorithm 6: Adaptive Tau Scheduling (Experiment 3)

Input: Target distribution p , Schedule $\{\tau_t\}_{t=1}^T$, Iterations T , Learning rate α **Output:** Optimized parameters θ^* , Loss history

```
1 Initialize  $\theta \leftarrow \{\mu = 0, \log \sigma = 0\};$   
2 Initialize Adam optimizer with learning rate  $\alpha;$   
3  $\mathcal{L}_{history} \leftarrow$  [];  
4 for  $t = 1$  to  $T$  do  
5    $\tau_t \leftarrow \text{schedule}[t];$  // Time-varying tau  
6    $\mathcal{L} \leftarrow \text{ComputeSRFELoss}(q_\theta, p, \tau_t, n=5000);$   
7    $g \leftarrow \nabla_\theta \mathcal{L};$   
8    $\theta \leftarrow \text{Adam.step}(\theta, g);$   
9   Append  $\mathcal{L}$  to  $\mathcal{L}_{history};$   
10 return  $\theta, \mathcal{L}_{history}$ 
```

Algorithm 7: Robustness to Outliers/Contamination (Experiment 4)

Input: Outlier Weight $outlier_weight$, Tau values $\{\tau_k\}_{k=1}^K$ **Output:** Metrics for each τ

```
1 Initialize  $p \leftarrow ContaminatedMixture(outlier\_weight=outlier\_weight)$ ;  
2  $results \leftarrow []$ ;  
3 for  $t = 1$  to  $K$  do  
4    $\tau_t \leftarrow schedule[t]$   $\mathcal{L} \leftarrow ComputeSRFELoss(q_\theta, p, \tau_t, n=5000)$ ;  
5    $metrics \leftarrow EvaluateApproximation(q_\theta, p, n_{eval}=10000)$ ;  
6   Append  $(outlier\_weight, \tau, metrics)$  to  $results$ ;  
7 return  $results$ 
```

Table 1: Experimental Configuration

Component	Configuration
<i>Target Distribution</i>	
Type	3-component Gaussian mixture
Means	$\mu_1 = (-3, 0), \mu_2 = (3, 0), \mu_3 = (0, 4)$
Covariance	$\Sigma = 0.5 \cdot I_2$ (shared)
Weights	$w = [0.3, 0.3, 0.4]$
<i>Variational Family</i>	
Type	Single Gaussian $q_\theta(x) = \mathcal{N}(x; \mu, \text{diag}(\sigma^2))$
Parameters	$\theta = \{\mu \in \mathbb{R}^2, \log \sigma \in \mathbb{R}^2\}$
Initialization	$\mu = 0, \sigma = 1$
<i>Optimization</i>	
Optimizer	Adam ($\beta_1 = 0.9, \beta_2 = 0.999$)
Learning rate	$\alpha = 0.05$
Iterations	$T = 2000$ (Exp 1-3), $T = 1500$ (Exp 4)
MC samples	$n = 5000$ per iteration
<i>Evaluation</i>	
ESS samples	$n_{eval} = 10,000$
Mode threshold	$0.01 \cdot \max_k q_\theta(m_k)$
Entropy samples	100,000 (for $H(p)$ estimation)
<i>Experiments</i>	
Exp 1: Methods	Forward KL, Reverse KL, SRFE ($\tau \in \{0.1, 0.3, 0.5, 0.7, 0.9\}$)
Exp 2: Tau sweep	$\tau \in [0.1, 0.9]$ (9 values), 3 trials each
Exp 3: Schedules	Fixed, Annealing, Reverse annealing, Stepwise
Exp 4: Outliers	Contamination: 0%, 10%, 20%, 30%

E EXPERIMENTAL RESULTS

The tables below contain a summary of the results from our empirical experiments. The best-performing cases (when relevant) are in bold.

From our results on Experiment 1 (Table 2), we see that the approximate distribution covers all three modes for SRFE with $\tau = \{0.3, 0.5, 0.7, 0.9\}$ and one mode for $\tau = 0.1$. Although we did not propose a method to determine the relative proportion of mass-covering and mode-seeking behavior based on the value of τ , our results indicate that the threshold occurs between $\tau = 0.1$ and 0.3 for this specific multimodal scenario. This is corroborated by the results from Experiment 2 as the average number of modes covered drops to 1 for $\tau = 0.1$ and 0.2 (Table 3). Furthermore, for all cases of τ , mode coverage is perfectly reproducible across trials (std = 0), indicating stable convergence of the objective (Table 4).

Table 2: Experiment 1 – Performance comparison of divergence measures on multimodal VI task

Method	Mode Coverage (out of 3) \uparrow	Entropy Error \downarrow	Test LogLik \uparrow	ESS \uparrow
Forward KL ($\tau \rightarrow 1$)	3	1.2232	-4.4727	2141.2888
SRFE ($\tau = 0.9$)	3	1.2984	-4.5134	2045.3491
SRFE ($\tau = 0.7$)	3	1.1252	-4.4556	2130.7683
SRFE ($\tau = 0.5$)	3	1.1209	-4.4815	2094.5110
SRFE ($\tau = 0.3$)	3	1.0225	-4.5039	1853.8958
SRFE ($\tau = 0.1$)	1	1.0986	-17.5261	3091.4211
Reverse KL ($\tau \rightarrow 0$)	2	0.4482	-7.1174	166.3425

Table 3: Experiment 2 – Performance comparison of SRFE at different τ values (avg. of metrics)

Method	Avg. Mode Coverage \uparrow	Avg. Entropy Error \downarrow	Avg. ESS \uparrow	Avg. Test LogLik \uparrow
SRFE ($\tau = 0.1$)	1	1.0929	7685.0161	-17.1385
SRFE ($\tau = 0.2$)	1	1.0738	6173.0793	-16.7109
SRFE ($\tau = 0.3$)	3	0.9969	1817.4306	-4.5164
SRFE ($\tau = 0.4$)	3	1.0979	2062.4072	-4.4815
SRFE ($\tau = 0.5$)	3	1.0871	2069.2320	-4.4624
SRFE ($\tau = 0.6$)	3	1.1537	2119.8005	-4.4656
SRFE ($\tau = 0.7$)	3	1.2016	2157.5103	-4.4723
SRFE ($\tau = 0.8$)	3	1.2746	2128.9023	-4.4605
SRFE ($\tau = 0.9$)	3	1.1711	2053.9186	-4.4573

Table 4: Experiment 2 – Performance comparison of SRFE at different τ values (std. of metrics)

Method	Mode Coverage Std.	Entropy Error Std.	ESS Std.	Test LogLik Std.
SRFE ($\tau = 0.1$)	0	0.0067	3254.3556	0.1807
SRFE ($\tau = 0.2$)	0	0.0132	3868.7299	0.2623
SRFE ($\tau = 0.3$)	0	0.0375	133.3366	0.0315
SRFE ($\tau = 0.4$)	0	0.0229	45.0580	0.0134
SRFE ($\tau = 0.5$)	0	0.0094	11.2182	0.0041
SRFE ($\tau = 0.6$)	0	0.0111	51.8966	0.0108
SRFE ($\tau = 0.7$)	0	0.0582	3.6637	0.0139
SRFE ($\tau = 0.8$)	0	0.0334	14.8822	0.0179
SRFE ($\tau = 0.9$)	0	0.0839	93.8879	0.0167

In Experiment 3, we evaluated the effect of simple scheduling strategies for τ based on the observation that the smooth forward-reverse KL divergence continuum captured by SRFE may allow it to gradually shift from mass-covering to mode-seeking behavior or vice versa by controlling τ . The effect of linear and stepwise schedules was tested; however, the effectiveness of the scheduling was inconclusive as the reported metrics are comparable across the tested strategies (Table 5).

Table 5: Experiment 3 – Performance comparison of fixed and annealing scheduling strategies

Method	Entropy Error ↓	Mode Coverage ↑	ESS ↑	Test LogLik ↑	Final Loss
Fixed $\tau = 0.5$	1.1721	3	2146.8315	-4.4581	1.7322
Fixed $\tau = 0.99$ (Forward KL)	1.3121	3	2060.4182	-4.5003	0.0000
Fixed $\tau = 0.01$ (Reverse KL)	0.4594	2	8.6457	-6.7723	2.6208
Annealing (0.3 → 0.9)	1.1561	3	2064.5593	-4.4414	1.0876
Reverse Annealing (0.9 → 0.3)	1.0088	3	1893.3969	-4.5421	2.0154
Stepwise (0.3 → 0.5 → 0.7 → 0.9)	1.2391	3	2093.3459	-4.4936	1.5042

In Experiment 4, we tested the performance of the SRFE objective at various levels of outlier contamination. Across the tested values objectives, higher values of τ corresponded with lower entropy error, higher effective samples size, and higher test log-likelihood, though the differences among those with the same levels of outlier contamination diminished as the contamination rate increased (Table 6).

Table 6: Experiment 4 – Performance comparison of SRFE at different τ values and outlier contamination.

Method	Outlier Weight	Entropy Error ↓	Mode Coverage ↑	ESS ↑	Test LogLik ↑
SRFE ($\tau = 0.01$)	0	0.4511	2	42.1605	-7.1755
SRFE ($\tau = 0.5$)	0	1.1326	3	2143.2493	-4.4626
SRFE ($\tau = 0.99$)	0	1.4338	3	1351.3932	-4.6495
SRFE ($\tau = 0.01$)	0.1	20.6654	3	4.8961	-23.0920
SRFE ($\tau = 0.5$)	0.1	21.0623	3	34.1576	-23.4870
SRFE ($\tau = 0.99$)	0.1	6.6339	3	24.1573	-9.2847
SRFE ($\tau = 0.01$)	0.2	20.3915	3	161.2464	-23.0292
SRFE ($\tau = 0.5$)	0.2	20.1851	3	24.5633	-22.8160
SRFE ($\tau = 0.99$)	0.2	18.9595	3	19.2893	-21.5955
SRFE ($\tau = 0.01$)	0.3	20.0987	3	9.3126	-22.9683
SRFE ($\tau = 0.5$)	0.3	19.8243	3	67.1477	-22.6946
SRFE ($\tau = 0.99$)	0.3	19.2067	3	133.3509	-22.0763